NASA CONTRACTOR REPORT

NASA CR-875

STUDIES OF MULTIVARIABLE MANUAL CONTROL SYSTEMS:

Two-Axis Compensatory Systems With Separated Displays and Controls

by William H. Levison and Jerome I. Elkind

Prepared by
BOLT BERANEK AND NEWMAN INC.
Cambridge, Mass.
for Ames Research Center

NATIONAL AERONAUTICS AND SPACE ADMINISTRATION • WASHINGTON, D. C. • OCTOBER 1967

NASA CR-875

STUDIES OF MULTIVARIABLE MANUAL CONTROL SYSTEMS:

Two-Axis Compensatory Systems With Separated Displays and Controls

By William H. Levison and Jerome I. Elkind

Issued by Originator as Report No. 1459

Prepared under Contract No. NAS 2-3080 by
BOLT BERANEK AND NEWMAN INC.
Cambridge, Mass.

for Ames Research Center

NATIONAL AERONAUTICS AND SPACE ADMINISTRATION

For sale by the Clearinghouse for Federal Scientific and Technical Information
Springfield, Virginia 22151 – CFSTI price $3.00

TABLE OF CONTENTS

TABLE OF CONTENTS (Cont.)

TABLE OF CONTENTS (Cont.)

TABLE OF CONTENTS (Cont.)

ABSTRACT

The results of a current study of multi-variable manual control systems are presented. The objectives of this study are to investigate the human controller's behavior in multi-variable control situations and to develop models of the controller which take into account both the monitoring and the control functions that he typically performs in such systems.

A series of two-variable manual tracking experiments was performed in which subjects were required to view two separated displays and operate two control devices to control the system. Performance was measured as a function of the display separation, the forcing function bandwidth, the task difficulty and the controlled-element dynamics. Human controller describing functions, eye movement distributions, and normalized mean-squared tracking error were obtained. Measurements were obtained when a single variable was viewed foveally, when a single variable was viewed peripherally, and when both variables were controlled simultaneously.

The primary difference between the 1-axis foveal, 1-axis peripheral, and 2-axis human controller describing functions in all experiments was a difference in the low-frequency gain. These gain differences were generally consistent with the NMSE differences. Two-axis and peripheral tracking performance was degraded as the display separation was increased: the NMSE increased, the fractional remnant increased, and the controller's

gain decreased. There was no appreciable effect on the mean observation time. Bandwidth and plant dynamics had a non-uniform effect on performance. The subject's allocation of foveal attention was affected by the relative task difficulties. The fraction of foveal attention devoted to an axis was on the average equal to the fraction of the total 2-axis mean squared error appearing on that axis.

A simple switching model of the human controller predicts with reasonable accuracy the effects of visual scanning on system performance. The key assumption of this model is that the human controller acts as a two-channel processor of information: one channel processes information foveally while the other simultaneously processes information obtained peripherally. There is assumed to be no coupling, or interference, between channels. A model of this type, coupled with a suitable model of the controller's monitoring behavior, should provide a means for extending current single-variable models of the human controller to multi-variable systems.

I. INTRODUCTION

Past studies of manual control systems have resulted in mathematical models of the human controller that provide accurate predictions of his behavior over a wide range of single-axis control situations (Refs. 1-3). Most systems of practical importance, however, are multivariable systems which generally require the human controller to time-share his visual attention and motor effort among a number of displays and controls. Although a number of studies comparing human performance in one- and two-axis control situations have been performed over the past few years (Refs. 4-11), there are presently no adequate models of the human controller applicable to a complex, multivariable situation.

The main objective of the research discussed in this report was to develop a model of the human controller that would predict controller and system performance in a two-axis system having separate displays and controls. This system was chosen for investigation because it contained two essential features of complex control systems -- multiple axes of control and sharing of visual attention -- and yet was simple enough to permit detailed and carefully controlled experimental study. This research program was the second phase of a continuing theoretical and experimental study of multivariable manual control systems. The first phase of the study, in which we investigated a two-axis control situation with integrated control and display, has been reported in detail in Ref. 10.

Our theoretical and experimental strategy was to build on the existing single-variable models of the human controller. Most of the experiments were structured so that comparisons could easily be made of the controller's performance on the 1-axis foveal task (the conventional tracking situation), the 1-axis peripheral task, and the 2-axis task. Primary experimental variables were (1) the display separation, (2) the forcing-function cutoff frequency, (3) the controlled-element dynamics, and (4) the heterogeneity of the left- and right-hand tasks. To the best of our knowledge, this report is the first to present human controller describing functions obtained during a purely peripheral tracking task or obtained in a multi-axis control situation requiring visual scanning.

In Chapter II of this report we review briefly the current status of models of the human controller and human monitor. The experimental program is described in Chapter III. Section A of that chapter contains a description of the apparatus and procedures common to most of the experiments. The experimental conditions investigated in the individual experiments, along with the training and data-taking procedures followed, are described in Section B. The analysis methods used and the performance measures obtained are discussed in Chapter IV. The experimental results are presented in Chapter V. In Chapter VI we discuss these results and suggest a model, based on current single-variable models, that will provide a good representation of the human controller in a two-axis compensatory control situation with separated controls and displays.

II. BACKGROUND

A. The Human Controller in Single-Variable Manual Control Systems

1. Describing Function Representations

In Fig. 1 is a block diagram of a flight control system. The pilot views a display and responds to the information displayed on it by moving the control device. The control device provides signals to the vehicle (controlled element) whose dynamics are represented by the transfer function C(s). Information about the response of the vehicle is processed and fed back to the display.

Most of the describing function studies have been performed with a compensatory display in which the displacement of the single indicator, the dot, is proportional to the tracking error. The human controller's task is to move the control device so as to correct or to compensate for this error. If the dynamics of the control device are negligible compared to those of the hand or arm, if the display is compensatory, and if the displayed error is the only stimulus to the operator, the dynamic characteristics of the system of Fig. 1 can be represented by the simpler block diagram of Fig. 2. The dynamic characteristics of the human pilot, which are nonlinear, noisy, and time-varying, can be represented by a quasi-linear operator H(s) (the describing function) and a remnant noise $n_h(t)$, added to the output of H(s).

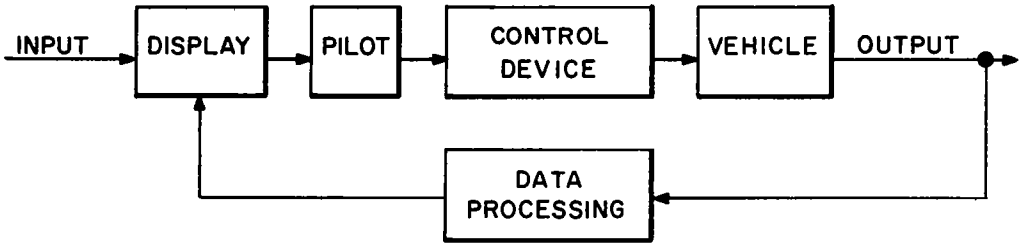

Fig. 1 Block Diagram of Single-axis Manned Flight Control System

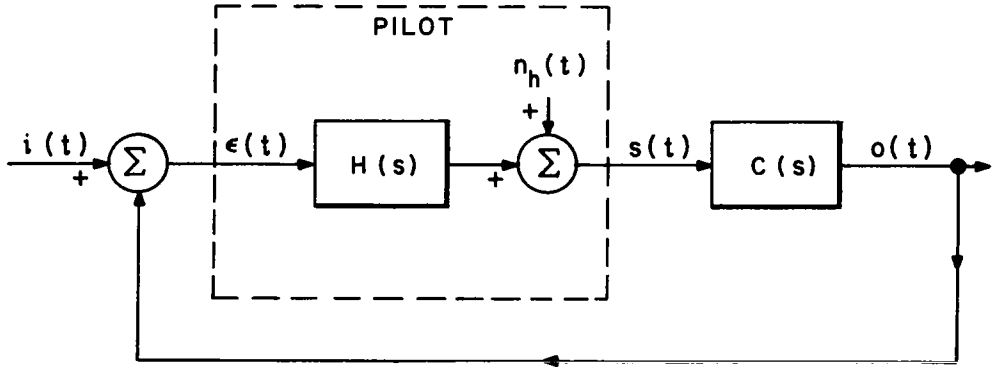

Fig. 2 Linearized Block Diagram of Flight Control System

2. Mathematical Models

The most comprehensive discussion of single-variable models of the human controller appears in McRuer et al (Ref. 3). They offer models of varying degrees of complexity to describe human control behavior in a wide variety of tracking tasks.

The simplest model states that the human controller adjusts his characteristics so that the combined pilot-vehicle describing functions will have a gain that decreases at a rate of 20 dB/decade in the region of gain crossover (the frequency at which $HC(j\omega) = 0$ dB). Thus

$$HC(j\omega) = \frac{\omega_c e^{-j\omega\tau_e}}{j\omega} \tag{1}$$

where ω_c is the gain crossover frequency and τ_ℓ is an effective time delay which includes neural conduction time, central processing time, and the effects of high-frequency poles. Although this model is intended to be valid only in the region of the gain crossover frequency, it is useful for predicting system performance, since a large fraction of the spectrum of the tracking error is often concentrated in a narrow frequency range that encompasses the gain-crossover frequency.

The gain crossover model implies that the human controller adapts his dynamic behavior to that of the controlled

element so that HC remains approximately constant, at least in the region of crossover.

A simple describing-function model that illustrates explicitly the adaptive capabilities of the human controller is:

$$H(s) = K_h \frac{(T_L s + 1)}{(T_I s + 1)} \cdot \frac{e^{-\tau s}}{(T_N s + 1)} \qquad (2)$$

The lead-lag term $(T_L s + 1)/(T_I s + 1)$ is an equalizer which together with the gain K_h is adjusted by the human controller to achieve good system performance. The delay τ and the lag $1/(T_N s + 1)$ approximate the dynamic characteristics of the neuro-muscular system. Experimentally-obtained estimates of τ are in the neighborhood of 0.09 second. When tracking with controlled-element dynamics of K, the controller generates a small lead time constant of about .11 sec, which has the effect of cancelling the effects of the neuro-muscular lag. He also employs a lag time constant and a gain K_h such that the gain crossover frequency is in the neighborhood of 8 rad/sec. When tracking with K/s dynamics, the controller no longer needs to generate a lag term T_I. He may attempt to generate a small lead time constant T_L, and he typically achieves a gain-crossover frequency of 5-6 rad/sec. When tracking with K/s^2 dynamics, the controller generates a lead time constant of about 5 sec, has a

neuro-muscular time constant T_N of about .11 sec, and essentially no equalizer lag T_I. He adjusts the gain K_h to achieve a gain crossover frequency of 3-4 rad/sec.

B. Models of the Human Controller of Multi-Axis Systems

1. Visual Scanning Not Required

Most studies of multi-axis manual control systems have focused on measures of system performance, such as mean-squared tracking error, rather than on descriptive measures of the human controller (Refs. 4-7). Two-axis human controller describing functions have been reported only recently, and these were obtained in control situations requiring no sharing of visual attention (Refs. 8-10).

In a previous study we compared 1-axis and 2-axis performance as a function of input bandwidth and as a function of task differences in a two-axis situation with integrated control and display (Ref. 10). Two types of differences were investigated: (1) different input bandwidths, and (2) different controlled-element dynamics.

We found that after considerable training the subjects were able to track two axes almost as well as one axis when the control situation was homogeneous. The two-axis normalized mean-squared tracking error (NMSE) was on the average about only 10% greater in the two-axis situation, and the one- and two-axis describing functions were nearly identical. Bandwidth had no consistent effect on these relationships.

Most of the increase in error could be attributed to an increase in remnant which we think may have resulted from an inadvertent and random coupling of the movements between the two axes. Since the source of this coupling could have resided in the visual system, the motor system, or in the intervening central pathways, we called this effect "visual-motor interaction."

When the tasks on the two axes were of unequal difficulty, the subjects appeared to concentrate more on the harder task with the result that the error increased much more in the easier of the two axes. This was an appropriate strategy for the subjects to follow, since they had been instructed only to minimize the total mean-squared error. If we consider only the sum of the mean-squared errors on the two axes, we find that 2-axis performance was nearly the same as 1-axis performance when the dynamics in the two axes were the same, including the situation in which the input bandwidths were different.

When the dynamics in the two axes were different, large increases in NMSE and appreciable changes in describing functions were observed. These observations are consistent with the results of others (Refs. 5-8). In our studies the dynamics were K on one axis and K/s^2 on the other. The NMSE nearly doubled on the K axis and increased by about 60 percent on the K/s^2 axis in the 2-axis control situation. The describing functions showed a decrease in gain at nearly

all frequencies, particularly on the K axis. Furthermore, the describing function on the K axis appeared to adopt some of the characteristics of the describing function on the K/s^2 axis. From these results we concluded that the requirement of the human controller to generate two different kinds of equalizer characteristics simultaneously was a direct cause of performance degradation.

In these integrated control-display studies we isolated three factors that appear to be sources of the deterioration in performance observed in two-axis tasks: visual-motor interaction, differential concentration on the two tasks, and the requirement to generate different equalizations. These experiments also provide evidence that certain factors do not have an important effect on two-axis performance. These are information transmission limitations and single-channel processing constraints. It is clear that the human controller does not operate at the limit of his information transmission capability in a single-axis task, since we found that he transmits almost twice as much information in certain two-axis tasks -- those in which the dynamics on the two axes are the same -- as he does in a single-axis task. The fact that the human controller can perform about as well in each axis of some two-axis tasks implies that he can process both channels of information in parallel rather than sequentially when provided with an integrated control-display configuration. Furthermore, we found no evidence in the describing functions of a switching mechanism for sequential processing, which further suggests that the two channels are processed in parallel.

2. Visual Scanning Required

Wierwille and Gagne (Ref. 11) measured time-varying transfer characteristics (mathematically equivalent to describing functions) of the human controller in one- and two-axis tracking situations. The two-axis tracking error was displayed oscillographically in one experiment via a single dot free to move in two dimensions, and in another by two meter movements separated by an amount sufficient to require visual scanning. The authors found the time-variability of the transfer characteristics was greater when the displays were separated than when they were integrated. One interpretation of this result is that the strategy applied to a given axis changed as the controller switched from foveal to peripheral viewing. The authors did not quantify the effects of visual scanning on the transfer characteristic.

Fitts and Simon (Ref. 4) also investigated a two-axis tracking situation in which the tracking errors were provided by two spatially separated meter movements. Time-on-target performance was continuously degraded as the display separation increased. (No descriptors of the human controller were computed.) The authors concluded that peripheral vision provided information for accurate eye movements and possibly for control movements.

C. Models of the Human Monitor

1. Multi-axis Monitoring Situations

Senders (Ref. 12) has formulated the following relationship between the monitoring behavior of the human observer and the characteristics of the signals displayed:

$$T_i = 2KW_i \operatorname{Log}_2 \frac{A_i}{E_i} + 2W_i C \qquad (3)$$

where T_i is the fraction of total time spent on instrument i, A_i is related to the range of instrument readings possible, E_i is a measure of the required accuracy of the reading, W_i is the bandwidth of the disturbance, and C and K are constants related to the individual's information processing and sampling capabilities.

The above model was tested experimentally in a multi-stimulus monitoring task in which no control effort was required. Random signals were presented via four or more meters separated so that only one at a time could be viewed foveally, and the subjects were required to respond to an out-of-bounds condition on one or more meters. The fraction of time devoted to a signal increased with the bandwidth of the signal, as predicted by Eq. 3. The fractional allocation of attention was adjusted primarily by variations in the fixation frequency. Mean observation time varied little and generally ranged from 0.3 to 0.4 seconds per look.

Although the model given by Eq. 3 was originally intended for a purely monitoring situation, Senders claims that it is also appropriate to a tracking situation if we interpret E_i as the permissible rms tracking error, A_i as the rms input, and W_i as the bandwidth of the error signal (Ref. 24). The model then predicts that the amount of visual attention devoted to a tracking display will increase as the bandwidth of the displayed signal increases and as the permissible NMSE is decreased.

Sanders (Ref. 13) investigated monitoring performance as a function of the separation between displays. In one of his experiments the subjects were presented with strings of dots projected at equal and opposite visual angles with respect to the median plane. The subjects depressed one of four keys, according to the combination of dots presented. The task was self-paced, and performance was measured as the number of responses in a given period of time. As expected from the results of Fitts and Simon (Ref. 4), performance decreased monotonically as the display angle was increased. Of particular interest, however, were the sharp performance drops that occurred between 20 and 40 degrees and again between 80 and 95 degrees.

On the basis of this and other experiments, Sanders proposed the following three functional levels of the visual field: (1) the stationary field, the display angle within which a task can be performed via peripheral vision, (2) the eyefield, in which eye movements (but not head movements) are necessary for satisfactory performance, and (3) the headfield,

in which head movements are required. Sanders attributed the unexpectedly large stationary field that he measured -- about 30 degrees -- to the low information content of the experimental task and predicted that the stationary field would shrink as the complexity of the task increased.

Sanders concluded from further experimentation with left-right discrimination tasks that the subjects processed information from both tasks before eye movements were made. This hypothesis is consistent with the conclusion of Fitts and Simon that peripheral cues were utilized in a 2-axis tracking task.

2. Peripheral Vision

The use of peripheral vision in monitoring and tracking performance has been inferred from the results discussed above. Additional studies have been made to evaluate directly the importance of peripheral vision (Refs. 13-15). Sanders (Ref. 13) required the subjects to view the stimulus both peripherally and during eye movements. Performance was better with peripheral viewing than with viewing during eye movements, and it was better than chance in both cases. Senders (Ref. 14) found that the detection of dial readings was better than chance for display angles as great as 80°.

The ability to utilize information from a signal source located at a given angle into the periphery depends on the precise location of the source and upon the type of motion. Fitts and Simon (Ref. 4) showed that a horizontal arrangement

of meters yielded better performance than a vertical arrangement for a given display separation. McColgin (Ref. 15) measured thresholds to peripheral motion as a function of both the location and the direction of motion and obtained results consistent with those of Fitts and Simon. He found that the threshold to motion located on the horizontal axis was only about half the threshold to motions located the same distance into the periphery on the vertical axis. In addition, he found that the threshold to vertically-directed linear motion was slightly (10-20%) but significantly less than the threshold to horizontally-directed motion when the signal source was located peripherally along the horizontal axis.

Additional factors affecting peripheral thresholds are: (a) brightness of object, (b) observation time, (c) size of object, and (d) structure of the visual background (Ref. 16).

D. Inadequacies of the Current Models

In order to discuss intelligently the inadequacies of the current models of the human controller, we should first determine the structure of a model that will adequately describe the behavior of the human controller in multi-axis control situations. A model for uncoupled axes should include: (a) a set of 1-axis models, one for each task; (b) a model of the sampling behavior which, for example, might be a process that adjusts the scanning pattern to optimize system performance in terms of the task criteria; and (c) a method of combining the single-axis models with the sampling model to predict multi-axis tracking performance. Parts (b) and (c) of the multi-axis model will be highly interactive.

Although various components of the multi-axis model have been investigated, there is no way at present to construct a unified model. Part (a) is presently available, thanks primarily to McRuer et al (Ref. 3). The sampling model of Senders (Ref. 12) may be applicable to part (b), but it has not yet been verified in a tracking situation. No models are currently available which enable one to predict the effects of sampling on the behavior of the human controller. The research described in this report was conducted primarily to provide a basis for the construction of such models.

III. EXPERIMENTAL PROGRAM

Section A of this chapter describes the apparatus and procedures used throughout the experimental program. The experimental conditions investigated in individual experiments, along with a description of the training procedures employed, are described in Section B.

A. Description of Apparatus and Procedures

1. The Basic Task

The human controller was presented with two compensatory tracking displays each of which contained a single error dot and a stationary reference circle of fixed diameter. In all except some preliminary experiments, the dots moved vertically and were controlled by compatible movements of two single-axis control sticks. Figure 3 shows a linear signal-flow diagram of the system. The controlled elements for each axis were simulated on a Goodyear Aircraft GEDA L3 analog computer; mean-squared tracking errors and other scoring and recording operations were performed on an Electronic Associates Inc. TR-48 analog computer. A digital Equipment Company PDP-1b digital computer was used to generate the forcing functions.

2. Displays and Controls

The displays and controls were located in a subject booth that was isolated acoustically and visually. A photograph of the subject booth is shown in Fig. 4. Each display was

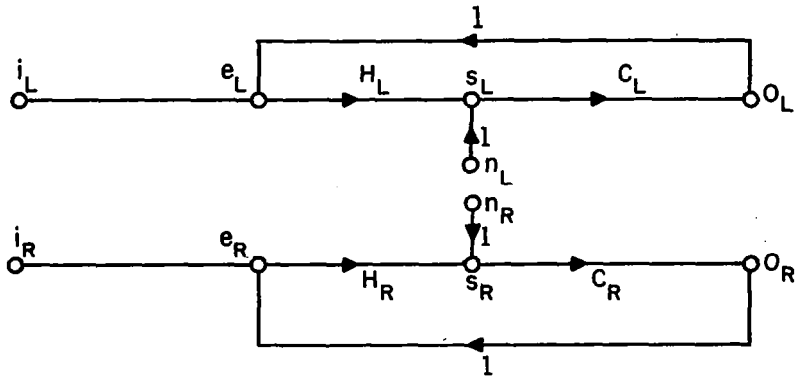

Fig. 3 Linear Flow Diagram of The Two-axis Compensatory Tracking System

The system input is represented by i. The portions of the system output, system error, and control movement linearly correlated with the input are designated respectively by o, e, and s. The controller's remnant is designated by n. H and C represent the controller's describing function and the controlled-element dynamics.

Fig. 4 Subject Booth

presented on the face of an oscilloscope of 12-cm diameter. An overlaid reticle provided a rectangular array of grid lines separated by approximately 1/2 cm. The distance between the subject's eyes and the plane of the displays was fixed at 72 cm. Lateral angular separations of 0.8°, 30°, or 56° about the median plane were used. A headrest was provided to minimize head motions. An electrophotometer was used to assure that there were no left-right differences between either the display or the scope background intensities. Intensity levels were consistent throughout the entire experimental program.

In all except a few preliminary experiments the subject manipulated two aluminum sticks, each of which was attached to a force-sensitive hand control (Measurement Systems Hand Control, Model 435). The tips of the control sticks protruded approximately 30 cm beyond the plane of the display. The subject used wrist and finger motions to manipulate the sticks and was provided with arm rests to support his forearms.

In order to provide a high degree of control-display compatibility, each control was oriented so that the stick was horizontal and could be moved in a plane parallel to the scope face. The response of the error dot to a deflection of the stick was in the same direction as the stick motion. The stick-control combination provided an omni-directional spring restraint with a restoring force of about 8×10^5 dynes per centimeter deflection of the tip of the stick.

The transducer of each hand control provided two independent electrical outputs, one proportional to the horizontal and the other proportional to the vertical component of

deflection. The sticks were allowed to move freely in both axes in all experiments. The error dots in the inactive axes were clamped electronically at zero displacement.

3. Eye Movements

Eye movements were monitored via electrooculographic techniques (Ref. 17). Voltages proportional to the horizontal deflection of the eyes were detected via Beckman biopotential skin electrodes and preamplified by an Electro Instruments Model A20B DC amplifier.

4. Controlled-Element Dynamics

The controlled-element dynamics were the same for both axes and were either pure gain (2×10^{-5} cm error displacement per dyne of stick force), velocity (8×10^{-5} cm/sec error displacement per dyne), or acceleration (8×10^{-5} cm/sec^2 error displacement per dyne).

5. Forcing Functions

Forcing functions were provided via a multi-channel FM magnetic tape system during training and were generated by a digital computer during the data-taking sessions. Seventeen sinusoids were summed to provide signals that were pseudo-Gaussian and whose spectra were rectangular, augmented by a high-frequency shelf. The cutoff frequency of the primary component was either 0.5, 1.0, or 2.0 rad/sec and the high-frequency shelf extended to 16 rad/sec. The shelf contained 0.5 percent of the total signal power. In order to assure orthogonality among the component sinusoids, an integral number

of cycles of each component was contained in the measurement interval (about 180 seconds). Thus, each component was a harmonic of the fundamental frequency

$$\omega_o = 2\pi/180 = .035 \text{ rad/sec.}$$

Table 1 gives for each component of the input the radian frequency and the number of wavelengths contained in the measurement interval. Also shown are the number of sum or difference frequencies of any two input components that coincide with each of the input frequencies. The set of frequencies chosen represents a compromise between the goals of providing a uniform logarithmic spacing between frequencies and of minimizing the coincidences with sum and difference frequencies.

We desired a flat input spectrum in order to relate our results to those obtained in our previous experimental programs and to simplify theoreticl calculations. In order to simulate a flat spectrum (referred to a linear frequency scale) with a set of sinusoids spaced equally on a logarithmic frequency scale, we adjusted the power levels of the components of the main signal to be proportional to frequency. We assigned identical power levels to each shelf component, however, so that: (1) measurements of nearly equal quality could be obtained at each shelf frequency, and (2) the controller's tracking performance would not be distorted by a disproportionately high power level at the highest shelf frequency. A typical continuous input spectrum equivalent to the discrete spectra used in these experiments is shown in Fig. 5.

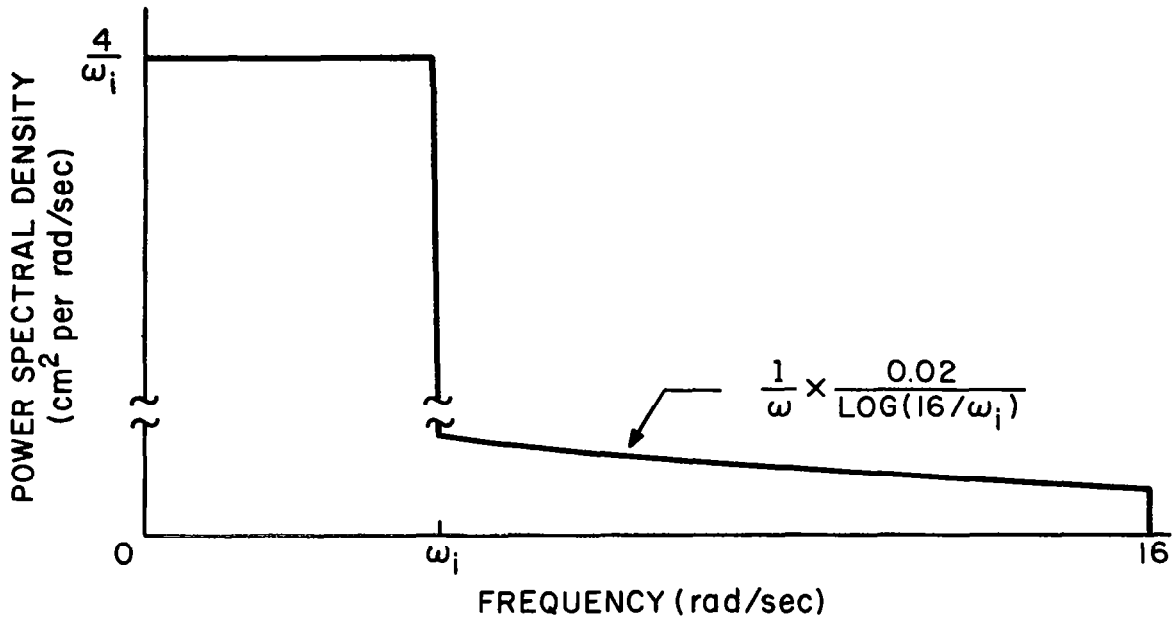

Fig. 5 Power Spectral Density of a Forcing Function Having A Nominal Bandwidth of ω_i Radians per Second

TABLE 1

Experimental Forcing-Function Frequencies

Number of wavelengths in measurement interval	Frequency (rad/sec)	Coincidences with sums and differences
2	0.07	3
3	0.11	3
4	0.14	2
5	0.17	3
7	0.24	3
12	0.42	2
15	0.52	1
21	0.73	0
29	1.0	0
39	1.4	0
57	2.0	1
83	2.9	0
114	4.0	1
160	5.6	0
233	8.1	0
330	12.	0
457	16.	0

Unless otherwise specified in Section B of this chapter, the experiments were designed so that the right-and left-hand single-axis tasks were equally difficult. In order to assure that the right and left forcing-functions were statistically identical over the measurement interval, the two signals were constructed to be the reverse of one another, with the possibility of a sign inversion. That is, if the left-hand forcing-function was $i_L(t)$ over the measurement interval $0 \leq t \leq T$, the right-hand input was either $+i_L(T-t)$ or $-i_L(T-t)$ for $0 \leq t \leq T$.

6. Instructions

The subjects were instructed to minimize the mean-squared tracking error. When tracking two axes, they were instructed to minimize the sum of the mean-squared errors on the two axes. The subjects were informed of their normalized mean-squared error performance after each session. Complete histories of the performance of all subjects were posted and shown to each subject in an attempt to foster a spirit of competition.

7. Subjects

Four subjects, all of them rated Air Force pilots, participated in the various phases of the experimental program. All subjects were currently active in the Air National Guard and were required to fly a minimum of 15-20 hours per month. Table 2 contains a brief history of the subjects' military and flying experience.

TABLE 2

Brief History of Pilots

Subject	Age	Flight Experiment (Hours)
JF	41	5600
DM	42	7000
PM	41	5200
CR	42	3800

8. Training and Experimental Procedure

All training and experimental trials lasted four minutes and were generally presented in sessions of three trials each with a fifteen-minute rest between sessions. The experimental sessions consisted of either three 1-axis trials, one 2-axis and two 1-axis trials, or one 1-axis and two 2-axis trials, depending on the requirements of the experiments. All mean-squared error scores and Bode plots were obtained from three-minute samples beginning 30 seconds after the onset of the forcing function. The subjects were trained under each condition until an apparently stable performance level was achieved.

A number of forcing-function waveforms were used during training under a given condition to minimize learning of the input. In order to minimize the variation of the experimental

results, however, a single pair of forcing functions was designated for each bandwidth condition and used for all data-taking.

9. Experimental Variables

In the preliminary experiments we intestigated (1) the number of controls (one 2-axis control or two 1-axis controls) and (2) the direction of the error dot and control movements (both axes vertically active, or left axis vertically active and the right axis horizontally active). A control-display configuration of two displays and two 1-axis controls active in the vertical axis only was chosen for the formal experimental program. The variables investigated in the formal experiments were (1) the separation between displays, (2) the mode of tracking (1-axis foveal, 1-axis peripheral, and 2-axis), (3) the input bandwidth, (4) the controlled-element dynamics, and (5) the mean-squared input. Table 3 indicates the range of variables used in each of the experiments.

B. The Experimental Program

The experimental program consisted of a set of preliminary experiments and four main experiments. Prior to the preliminary experiments the subjects were given extensive training. We describe this training period first and then discuss the experimental conditions and the training and data-taking procedures for each of the experiments.

It was not possible to maintain a predetermined schedule of training and experimentation over the four-month period spanned by the formal experimental program. In addition,

TABLE 3

Experimental Variables

Experiment	Number of Controls	Type of Display	Display Separation (degrees)	Mode of Tracking	Plant Dynamics (cm/dyne x 10^{-5})	Input BW (rad/sec)		MSI (cm^2)	
						Axis A	Axis B	Axis A	Axis B
Preliminary	1, 2	V-H V-V	30	1-axis 2-axis	8/s	2	2	4	4
Experiment 1	2	V-V	.8, 30, 56	1-axis 2-axis peripheral	8/s	2	2	4	4
Experiment 2	2	V-V	30	1-axis 2-axis peripheral	8/s	.5 1 2	.5 1 2	32 16 4	32 16 4
Experiment 3	2	V-V	30	1-axis 2-axis		.5 .5 .5 2	.5 2 2 2	32 16 4 4	32 4 4 4
Experiment 4	2	V-V	30	1-axis 2-axis peripheral	2 8/s 8/s2	1	1	16 4 10	16 4 10

we modified our experimental plans as new knowledge was gained. For these reasons the training and experimental sessions were not entirely carried out in what we now conceive to be the proper logical order. Deviations from this order are noted below in the discussion of the individual experiments.

1. Initial Training

The subjects were trained first on single-axis horizontal and vertical tasks until they appeared to reach a stable level of performance. The controlled-element dynamics were K_1/s, the forcing-function bandwidth was 1.5 rad/sec, and the MSI was 4 cm^2.* A typical training record is shown in Fig. 6. Each entry represents the average score from three 4-minute tracking runs. The entire record represents 48 runs or a total of 192 minutes of tracking.

After achieving a stable one-axis performance level, the subjects trained on a mixture of one-axis and two-axis tasks with a display separation of 30 degrees. Each training session contained a horizontal-axis (H-axis), a vertical-axis (V-axis), and a two-axis trial, presented in a balanced order. The subjects practiced first with a 1.5 rad/sec input, then with the 2.5 rad/sec forcing function.** In alternate training sessions the subjects used two 1-axis control and one 2-axis control. An average of 90 runs per subject were devoted to this phase of the training. The results of the final two days of training are shown

---

* $K_1 = 8 \times 10^{-5}$ cm/sec of display displacement per dyne of applicable force.

** The forcing functions used for initial training and for the first preliminary experiment were of the type described in Ref. 10. All subsequent experiments used the forcing functions described earlier in this section.

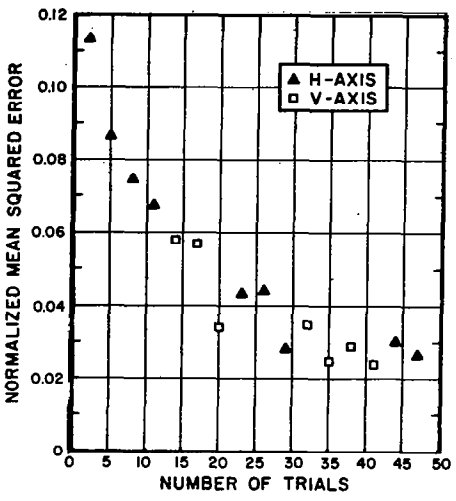

Fig. 6 Initial 1-axis Training Record

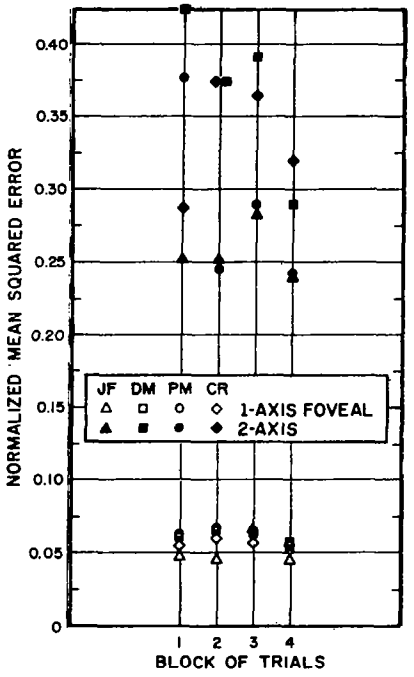

Fig. 7 Initial 2-axis Training Record

in Fig. 7. Each data point represents the average of four trials, one from each axis for each control configuration.

2. Preliminary Experiments

The first preliminary experiment was conducted to help us decide whether to provide the subjects with a single 2-axis control or with two 1-axis controls for the formal experimental program. Use of a single 2-axis control would have provided a link to our recent experimental program (Ref. 10) in which the subjects were provided with an integrated 2-axis display and an integrated 2-axis control. On the other hand, we suspected that there might be more visual-motor interference between axes with the 2-axis control (Ref. 7). We decided, therefore, to choose the control configuration that resulted in the best 2-axis NMSE performance.

Four subjects participated in this experiment. A vertical display of the left-hand error dot and reference circle and a horizontal display for the right-hand system were provided. The displays were separated by 30 degrees, the controlled-element dynamics were K_1/s, and each input signal had a bandwidth of 2.5 rad/sec and mean-squared level of 4 cm^2. Each data-taking session consisted of two single-axis runs, one for each axis, and one two-axis run, presented in a balanced order. Each subject tracked four sessions, two with each of the control configurations.

Two 1-axis controls resulted in the best NMSE performance and were therefore used for the remainder of the experimental program.

The next preliminary experiment was intended to test our experimental apparatus and procedure. The system was the same as in the previous experiments except that two 1-axis controls were used, the input waveform was generated by the digital computer and had a bandwidth of 2 rad/sec, and eye movements were recorded. We chose to use a combination of vertical movements in one control-display pair and horizontal movements in the other in order to be compatible with our previous experimental procedures (Ref 10) and because we suspected that there might be less chance of improperly relating controls to displays if the two control-display systems were spatially orthogonal. However, 2-axis tracking performance differed between the two axes by about 30%, and different amounts of visual attention were devoted to the two displays. To eliminate this source of asymmetry, we decided to use two vertically-active control-display systems in all subsequent experiments.

3. Main Experiments

(a) Experiment 1: Effects of Display Separation

The object of this experiment was to determine the effects of display separation upon the human controller's 1-axis peripheral and 2-axis behavior and upon system performance. An additional objective was to show that the difference between one-axis and two-axis performance was due primarily to the shift of foveal attention between displays, and not merely a result of tracking two axes simultaneously.

The subjects were provided with two vertically-active control-display systems for which the controlled elements were K_1/s, the input bandwidths were 2 rad/sec and the MS input levels were 4 cm^2. The display separations were 0.8°, 30°, and 56°.

The 0.8° display separation was obtained by displaying both error dots and reference circles on a single oscilloscope positioned directly in front of the subject. The two larger display separations were obtained as described in Section A of this chapter.

Both reference circles and error dots were displayed for all experiments, but one of the dots was clamped electronically at zero displacement during the 1-axis trials. When tracking peripherally, the subject fixated on the stationary dot.

The 0.8° separation was used so that the subject would be able to track the two error dots simultaneously without visual scanning. Any degradation in performance caused by the addition of the second axis of tracking was attributed to the requirement of tracking simultaneously in two axes without the benefit of an integrated control-display configuration. A further degradation in performance observed with the larger display separations could be attributed to the necessity of visual scanning. Separations of 30° and 56° were chosen because they spanned a range in which eye movements but not head movements are required (Ref 13).

One-axis foveal and 2-axis data were gathered from all four subjects. Because of illness, Subject DM was unable to participate in the peripheral-tracking phase of this experiment. The subjects first trained for an average of 42 runs total on the 1-axis foveal and the 2-axis tasks. Each training session contained two 2-axis trials and one 1-axis trial with an equal number of sessions devoted to each separation.

Each subject tracked for three data-taking sessions. The first session contained two 1-axis and two 2-axis tasks; the remaining sessions consisted of two 2-axis and one 1-axis tasks. Each session contained a different display separation, assigned in a balanced order among the subjects. Each subject performed two 1-axis runs on each axis and two 2-axis runs with each display separation.

After the 1-axis foveal and 2-axis data were gathered, each subject devoted about 40 training runs to the 1-axis peripheral task. Each session of three runs was conducted with a fixed display separation of either 30 or 56 degrees; left- and right-hand tasks were presented alternately.

Each subject tracked peripherally for four data sessions, two with each separation for a total of three trials per axis per separation. The sessions consisted of three trials total, with L and R tasks presented alternately. One display separation was used for the first two sessions and the other separation for the final two sessions. The order of separation was varied among the subjects. Eye-movement records obtained during data taking indicate that the subjects did not glance foveally at the moving dot.

(b) Experiment 2: Effects of Input Bandwidth

The object of this experiment was to investigate the effects of bandwidth on the relation between 1-axis foveal, 2-axis and 1-axis peripheral performance. The subjects were presented with two vertical control-display systems with homogeneous tasks. The display separation was maintained at 30° and the controlled elements were K_1/s. The input bandwidths were 0.5, 1, and 2 rad/sec, and the MSI's were, respectively, 32, 16, and 4 cm^2. The MSI of 4 cm^2 was selected for the 2 rad/sec bandwidth condition to be compatible with the preceding

experimental conditions. The remaining MSI's were chosen so that the 1-axis foveal mean squared errors would be roughly the same (about 0.2 cm^2) for all bandwidth conditions. Since subject CR was unable to continue beyond Experiment 1, this and the following experiments were conducted with the remaining three subjects.

The subjects trained first for an average of 50 runs/ subject total on the 1-axis foveal and 2-axis conditions. Bandwidth was varied between training sessions of three trials, and training was mostly on the 2-axis task.

Nine data runs were obtained from each subject for two consecutive evenings for a total of 18 runs per subject. Two sessions each were spent on the 0.5, the 1.0 and the 2.0 rad/sec bandwidth condition, in that order. Each session consisted of an L-, and R-, and a 2-axis trial, presented in a balanced order, all having the same input bandwidth.

Unfortunately, we did not obtain the corresponding 1-axis peripheral data until the subjects had been trained and tested on other conditions. Nevertheless, very little training was needed in this situation: an average of 6 trials were devoted to the 1 rad/sec input and 3 trials to the .5 rad/sec input. (The 2 rad/sec peripheral condition was not re-tested; appropriate data were obtained from Experiment 1.)

Each subject tracked peripherally for four data sessions, two with each bandwidth for a total of three 1-axis peripheral trials per axis per bandwidth. L- and R-axis tasks were presented alternately. One bandwidth was used for the first two sessions, and the other bandwidth for the remaining two sessions. The order of presentation of bandwidths was varied among subjects.

(c) Experiment 3: Effects of Axis Differences

The object of this experiment was to determine the allocations of mean squared error and foveal attention and to investigate modifications of the controller's describing function when the tracking tasks on the two axes were different. This experiment was divided into two parts. In the first part, only the input bandwidths were different. In the second part, the input bandwidths were different and the MSI's were adjusted so that the 1-axis foveal mean squared errors (unnormalized) would be nearly identical on the two axes.

Two vertically-active control-display systems were provided with a display separation of 30 degrees and with identical controlled elements of K_1/s. Bandwidths employed were 0.5 and 2 rad/sec. Data on the corresponding homogeneous tracking situations obtained from the preceding experiment were used for comparison.

Since the MSI was homogeneous in the first part of this experiment, the different input bandwidths resulted in different task difficulties on the two axes. An MSI of 4 cm^2 was chosen to provide a 1-axis foveal mean squared error of about 0.2 cm^2 on the high-bandwidth axis. An average of 45 training trials were provided each subject in this situation. Since only the two-axis task required learning, each training session consisted of two 2-axis trials and one 1-axis trial to provide a baseline check. Nearly equal numbers of trials were presented with the 0.5 rad/sec input on the left and the 2.0 rad/sec on the right axis, and vice versa, in order to average out the effects of possible left-right biases.

Four data sessions--a total of 12 trials--were obtained per subject. Each session consisted of the low-bandwidth task alone, the high-bandwidth task alone, and a two-axis task. The 2 rad/sec input appeared on one axis for the first two sessions and on the other axis for the remaining two sessions. The order of the axis-bandwidth combinations was varied among subjects.

In the next part of this experiment, the MSI to the low-bandwidth axis was increased to 16 cm^2 so that the 1-axis foveal mean squared error would be about .2 cm^2. The MSI to the high-bandwidth axis remained at 4 cm^2. Each subject trained for an average of 30 trials total under these conditions; the training and data-taking procedures were otherwise identical to those of the preceding phase.

(d) Experiment 4: Effects of Controlled-Element Dynamics

The object of this experiment was to determine the effects of controlled-element dynamics on the relation between 1-axis foveal, 1-axis peripheral, and 2-axis tracking performance. Two homogeneous, vertically-active control-display systems having a display separation of 30^o and input bandwidths of 1 rad/sec were used. The controlled-element dynamics were K, K/s, and K/s^2, and the MSI's were adjusted in each case to yield a 1-axis foveal MSE of about 0.2 cm^2.

The results of Experiment 2 were used to provide data for the K/s condition. The K/s^2 and K dynamics conditions, in that order, were investigated sequentially to complete the experimental program.

The subjects trained initially with controlled elements of $8x10^{-5}/s^2$ (K_1/s^2) cm/dyne and an input bandwidth of 2 rad/sec for 12 1-axis foveal trials. The subjects then attempted to track the two axes simultaneously, but were consistently unable to keep the error dot within the display limits of $\pm$ 6 cm for an entire 4-minute run.

The input bandwidth was then lowered to 1 rad/sec and the MSI was set at 4 cm^2. Fifteen additional training sessions were provided, each containing an L- and R-, and a 2-axis task for a total of 45 trials per subject. Ten of the 30 1-axis tasks were performed peripherally.

The subjects tracked four data sessions each. The first two sessions each contained an L-, and R-, and a 2-axis task, presented in a balanced order. The final two sessions each contained three 1-axis peripheral trials presented alternately on L and R.

After completion of the K/s^2 phase, the subjects were trained with controlled elements of $2x10^{-5}(K_1/4)$ cm/dyne, an input bandwidth of 1 rad/sec, and MSI of 10 cm^2. Nine training sessions of the type described above provided each subject with a total of 27 training runs. Three of the nine 1-axis tasks were performed peripherally. The data-taking procedure was identical to that described above.

IV. ANALYSIS TECHNIQUES

A. Descriptive Measures

1. Normalized Mean Squared Error

Normalized mean-squared error (NMSE) scores were computed for each of the one-axis runs and for each axis of the two-axis runs. Normalization was with respect to the mean-squared input (MSI) to the axis. In addition total-task NMSE scores were computed for the two-axis runs by normalization of the sum of the left and right MSE with respect to the sum of the MSI. The fraction of the total MSE allocated to each axis of each two-axis run was also computed.

Analyses of variance (Ref 18) were performed on the NMSE scores to determine the significance of the difference between the one-axis foveal and two-axis scores. When the experimental conditions were homogeneous, a separate analysis was conducted on the L-axis, R-axis, and total-task scores.* When the input bandwidths were different, analyses were performed for each bandwidth condition and for the total-task measure. The primary variables of these analyses of variance were the number of axes tracked and the subject.

---

* Pairs of left and right one-axis scores were averaged together to yield a one-axis measure to correspond to the two-axis total-task measure.

2. Eye-movement Statistics

The mean observation time and the fraction of foveal attention allocated to the axis were computed for each axis of each two-axis trial.* Also computed were the frequency distributions of the observation times for selected runs. Transition times were disregarded in the computation of these statistics; the subject was considered to be looking at either the left or right display at any instant of time.

3. Describing Functions

Human controller describing functions relating dynes of control effort to centimeters of error displacement were obtained using Fourier analysis techniques similar to those employed by Tustin (Ref 19), McRuer et. al. (Ref 3), and Taylor (Ref 20). The computational procedure was based on the Cooley-Tukey method of computing transforms (Ref 21). This computational procedure was embedded in the signal analyzer system developed by Grignetti, Payne and Elkind (Ref. 25). In order to optimize the signal-to-noise ratio, measurement frequencies and forcing-function frequencies were made to coincide.

4. Power Spectra

Selected power spectra were obtained using the Cooley-Tukey procedure. Each spectrum consisted of a set of lines spaced approximately by .035 rad/sec and extending from .035 to about 72 rad/sec. Measurements beyond 16 rad/sec were disregarded.

---

* We use the term "foveal attention" as a convenient designation of fixation of gaze. No other connotation of the word "attention" is implied.

5. Remnant

The "fractional remnant power" for a signal was defined as the portion of power in that signal not appearing at the forcing function frequencies normalized with respect to the total signal power. The remnant so defined was assumed to account for all of the signal power that was not linearly related to the forcing function.

B. Calibration of The Describing-Function Analysis Procedure

Describing functions were obtained for fixed, linear analog test filters imbedded in a control loop. The forcing-function bandwidth was 2 rad/sec. The controlled-element dynamics were K/s for the first set of simulation experiments, and the transfer function of the test filter was

$$H(s) = 1.4 \left[\frac{1}{1+s/8} \right]^3 \qquad (4)$$

Gaussian noise uncorrelated with the forcing function was added to the filter output to simulate stick remnant power. Three experiments were performed with this particular test filter. No remnant was added in the first experiment. In the second experiment, the simulated remnant accounted for 17% of the total simulated stick power and had a spectrum that was flat below 20 rad/sec and proportional to $1/\omega^2$ at higher frequencies. In the third experiment, the simulated remnant accounted for 24% of the total stick power and had a spectrum that was proportional to ω^2 below 10 rad/sec, flat between 10 and 20 rad/sec, and proportional to $1/\omega^2$ at higher frequencies.

The controlled-element dynamics were K/s^2 for the second set of calibration experiments, and the transfer function of the test filter was

$$H(s) + 2\ \frac{s+1/2}{s+4} \qquad (5)$$

Two experiments were performed with this filter--one without remnant, and one with a remnant spectrum proportional to ω^2. The remnant power constituted 25% of the simulated stick power in the second experiment.

The describing functions of the test filters obtained experimentally are given in Figure 8. Amplitude-ratio and phase-shift errors were generally less than 1 db and 10 degrees over the entire measurement range of 1/16 to 16 rad/sec when no remnant was simulated. (The largest fractional remnant power measured in this situation, about 5% is indicative of the noise level of the system.) Even when moderate amounts of remnant were simulated, AR and phase errors were less than 3 db and 20 degrees over most of the spectrum. Accuracies of 1 db and 10 degrees were obtained between .5 and 2 rad/sec, the frequency region containing most of the simulated stick power.

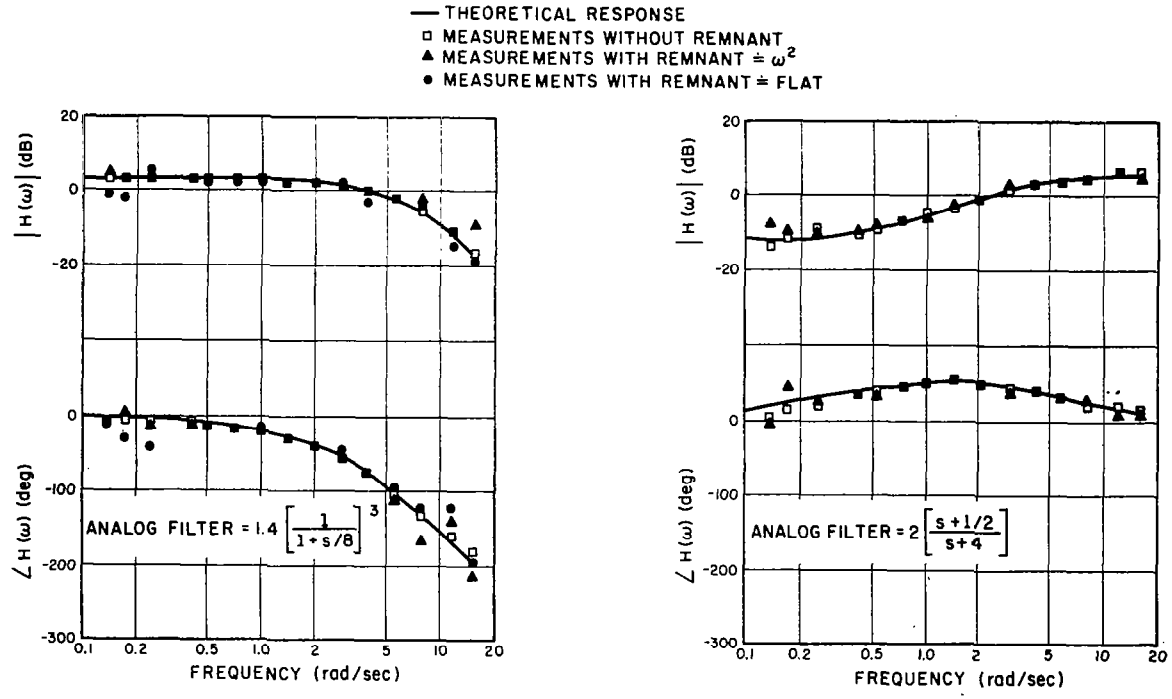

FRACTIONAL REMNANT POWER

	STICK	ERROR
NO REMNANT ADDED	0.032	0.048
WITH REMNANT ≐ ω^2	0.170	0.130
WITH REMNANT ≐ FLAT	0.240	0.280

FRACTIONAL REMNANT POWER

	STICK	ERROR
NO REMNANT ADDED	0.028	0.013
WITH REMNANT ≐ FLAT	0.252	0.022

Fig. 8 Closed Loop Calibration Test: Measured and Computed Transfer Functions of Test Filters

V. EXPERIMENTAL RESULTS

In this chapter we present the principal experimental results. Most of these are in the form of averages taken over subjects and over certain of the experimental conditions. The average performance of each subject under each experimental condition are tabulated in Appendix A, which contains Tables A1 through A19.

A. Preliminary Experiments

1. Effects of Controls

This experiment was conducted to determine whether two 1-axis controls or one 2-axis control would yield lower 2-axis NMSE scores. The 2-axis NMSE with the single control was 1.6 times that obtained with two 1-axis controls. An analysis of variance indicated that this difference was significant at the .001 level and that there was no interaction between subjects and controls.* The difference between the 1-axis foveal NMSE scores in the two situations was negligible--less than 10%.

Our result of lower scores with two controls differs from that of Chernickoff and LeMay (Ref. 7) who observed lower error scores with one control when the dynamics and the two axes were K/s^2 and essentially equal scores when they were K. There were several basic differences between our experiment and theirs, a principal

---

* Although many of the NMSE results are presented as percentage differences or ratios, all analyses of variance referred to in this report have been performed directly on the NMSE scores and indicate the statistical significance of the difference of these scores under various experimental conditions.

one being that they displayed the two dots on one display instead of on two displays. This may have allowed their subjects to generate coordinated responses on the two axes more easily than ours could.

We did not pursue the source of this difference since it was peripheral to our main interests, and decided to use the two-control configuration throughout the remainder of the experimental program because it led to lower NMSE scores.

2. Vertical-Horizontal Configuration

This experiment revealed that the horizontal task was more difficult than the vertical task in a 2-axis situation. The 2-axis NMSE scores were on the average 1.3 times greater on the horizontal (H) axis than on the vertical (V) axis (Table A1)* whereas the H-axis score was only about 10% greater in the 1-axis foveal tracking situation. The analysis of variance (Table A2) showed that both differences were significant at the 0.01 level. In addition, the superior V-axis performance was achieved in spite of the fact that the subjects attended to the V axis only 42% of the time (Table A3).

These results indicate that there was a difference in the difficulty of the H and V tasks in the 2-axis situation that cannot be accounted for entirely by a basic difference in the subjects' ability to track vertically and horizontally, nor by a left-right difference in tracking ability. In order to remove the vertical-horizontal asymmetry as a possible source of bias, the main experiments were conducted with two control-display systems active in the vertical dimension only.

---

* Tables A1 through A-19 are in the Appendix.

B. Main Experiments

1. Effects of Display Separation

In this experiment we investigated the effects of display separation on 2-axis and 1-axis peripheral tracking performance.

(a) NMSE Scores

The average NMSE scores for 1-axis foveal ($NMSE_f$), 1-axis peripheral ($NMSE_p$), and 2-axis ($NMSE_2$) tracking are shown in Table 4. Also shown in Table 4 are the quantity $\overline{NMSE_2/NMSE_f}$, the average of the ratios of 2-axis NMSE to 1-axis foveal NMSE, and the quantity $\overline{NMSE_p/NMSE_f}$, the average of the ratios of 1-axis peripheral NMSE to 1-axis foveal NMSE.* NMSE scores for the individual subjects are presented in Table 4.

The 2-axis and 1-axis peripheral performance was degraded markedly as the display separation was increased. However, even with a separation of 56°, the subjects were able to track with some degree of effectiveness using peripheral vision alone; an average NMSE of 0.80 resulted from these conditions.

The necessity to track two non-integrated axes simultaneously--even when both error dots could be viewed foveally most of the time--produced a significant increase in the NMSE. The $\overline{NMSE_2/NMSE_f}$ ratio of 1.5 observed with the display separation of 0.8° indicates the magnitude of this performance degradation. The $\overline{NMSE_2/NMSE_f}$ ratios of 3.9 and 8.9 observed with display separations of 30° and 56°, respectively, show the additional degradation due to visual scanning.

---

* The $NMSE_p/NMSE_f$ and $NMSE_2/NMSE_f$ ratios were computed for each subject and averaged together to yield the quantities $\overline{NMSE_p/NMSE_f}$ and $\overline{NMSE_2/NMSE_f}$.

TABLE 4

Effect of Display Separation on Mean-Squared Error, Remnant and Mean Observation Time

		Display Separation		
		0.8°	30°	56°
Normalized Mean-Squared Errors	$NMSE_f$	.050	.050	.050
	$NMSE_p$	—	.36	.80
	$NMSE_2$	.073	.19	.42
NMSE Ratios	$\overline{NMSE_2/NMSE_f}$	1.5	3.9	8.9
	$\overline{NMSE_p/NMSE_f}$	—	7.5	17
Fractional Remnant Stick Power	1-axis foveal	.17	.17	.17
	1-axis peripheral	—	.48	.65
	2-axis	.19	.40	.54
Fractional Remnant Error Power	1-axis foveal	.33	.33	.33
	1-axis peripheral	—	.70	.67
	2-axis	.34	.53	.58
Mean Observation Time (seconds)		—	1.2	1.3

Controlled-Element Dynamics: K/s
Input Bandwidth: 2 rad/sec
Subjects: JF, PM, CR: All conditions
DM: 1-axis foveal and 2-axis conditions

An analysis of variance (Table A5) showed that the differences between 1-axis foveal and 2-axis performance was generally significant at the .001 level. No analysis of variance was performed to test the differences between 1-axis foveal and peripheral scores; nevertheless, the significance is clear because the differences were large compared to the standard deviation of either the foveal or peripheral scores.

(b) Power Spectra

Stick and error power density spectra for one subject are shown in Figure 9 for the 1-axis foveal, 1-axis peripheral, and 2-axis tracking conditions. The display separation was 30^{o}. Power levels at each forcing frequency are indicated by the isolated symbols, and the connected line segments indicate the remnant power averaged over a quarter of an octave.

Figure 9a shows that the stick power at forcing frequencies below 2 rad/sec (the input cutoff frequency) increased at a rate of 30 dB per decade--20 dB more per decade than the input. This is the expected result with dynamics of K/s. The power levels at these forcing frequencies were nearly the same for the three tracking conditions.

The remnant power density spectrum, which was transformed into a step-wise continuous spectrum by the averaging process, increased at 20 dB/decade up to 5 rad/sec (the gain-crossover frequency for this experiment) and decreased at a rate of 20-30 dB/decade at higher frequencies. The highest and lowest remnant power density levels were observed, respectively, for the 1-axis peripheral and 1-axis foveal conditions. Since the stick power density at each forcing frequency was generally more than 10 dB

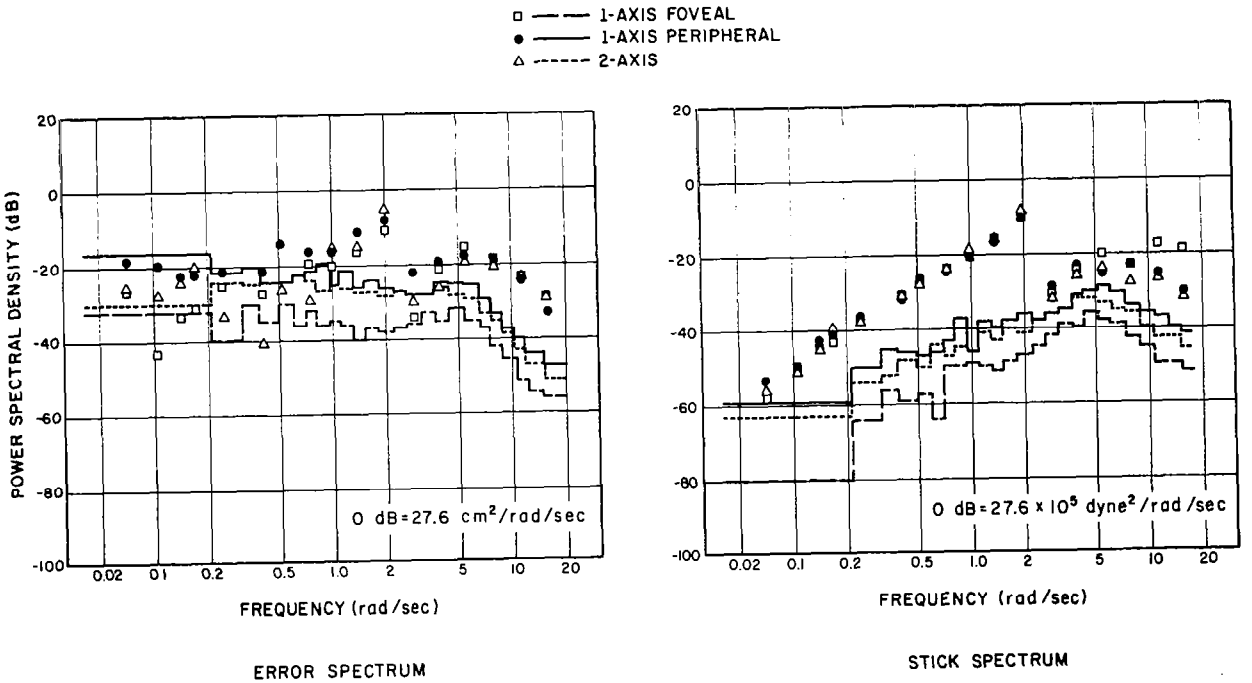

Fig. 9 Comparison of 1-axis Foveal, 1-axis Peripheral, and 2-axis Error and Stick Power Spectra

Controlled elements: K/s
Input bandwidths: 2 rad/sec
Display separation: 30 degrees
Subject: PM

above the remnant power density at neighboring frequencies, we can assume that measurements of the human controller's stick response at forcing frequencies were essentially uncorrupted by remnant. remnant.

Figure 9b shows that the error power at the forcing frequencies increased at the rate of 30 dB/decade between about 0.5 and 2 rad/sec. The shape of the spectrum was not well defined at lower frequencies. The remnant error spectrum was relatively flat out to 5 rad/sec and decreased at a rate of about 40 dB/decade at higher frequencies. The remnant error spectrum was thus equal to the remnant stick spectrum cascaded with $|K/s|^2$ the transfer function of the controlled-element, as expected.

The error power density at forcing frequencies below $\omega_i/8$ was generally less than the remnant power at neighboring frequencies. Because of the low signal-to-noise ratio, we cannot expect to have valid describing function measurements in this region of the spectrum. Therefore, describing function measurements presented in this report are not given for frequencies less than $\omega_i/8$.

(c) Describing Functions and Remnant

Figure 10 shows average human controller describing functions (DF) obtained from the left (L) and right (R) axes when the display separation was 30^o. The L and R describing functions were in very close agreement for both the 1-axis foveal and 2-axis tracking conditions. Since there were no important left-right describing function differences, describing function measurements were made on only the R axis in the remainder of the experimental program.

Figure 11 shows the effects of display separation on the 1-axis and 2-axis describing functions. The 0^o measurements

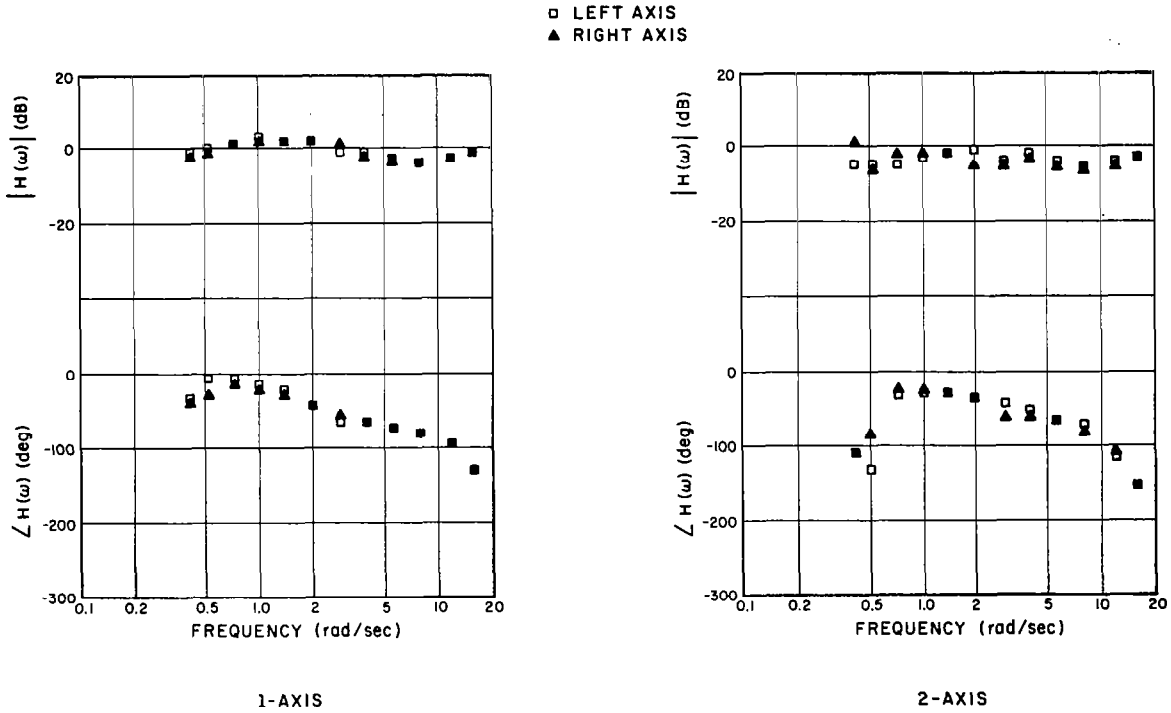

Fig. 10 Comparison of Left-axis and Right-axis Average Human Controller Describing Functions

Controlled elements: K/s
Input bandwidths: 2 rad/sec
Display separation: 30 degrees
Subjects: four

0 dB = 10^5 dynes/cm

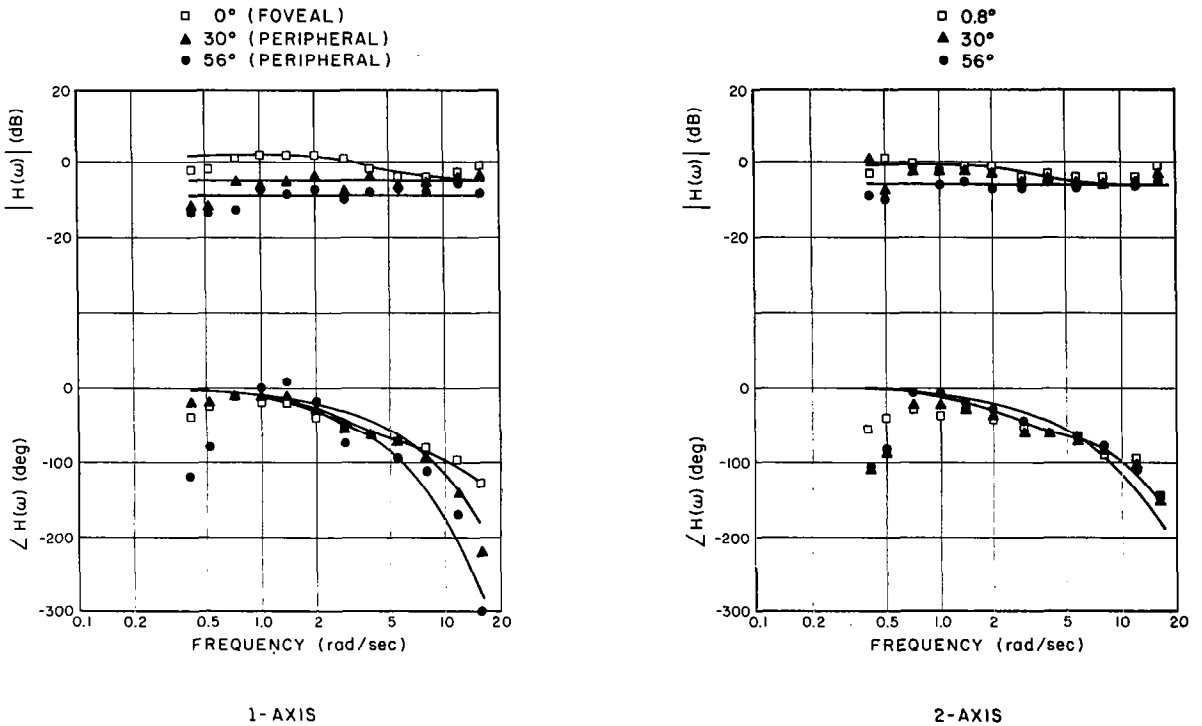

Fig. 11 Effects of Display Separation on Average Human Controller Describing Functions

Controlled elements: K/s
Input Bandwidths: 2 rad/sec
Subjects: four

0 dB = 10^5 dynes/cm

indicated in Figure 11a are for foveal tracking, whereas the 30° and 56° 1-axis measurements are for peripheral tracking.

The human controller describing functions have been approximated by transfer functions of the form

$$H(j\omega) = K_h \frac{1+j\frac{\omega}{\omega_2}}{1+j\frac{\omega}{\omega_1}} e^{-j\omega\tau} \qquad (6)$$

where K_h is the low-frequency gain, τ the controller's effective time delay, and ω_1 and ω_2 are parameters of the equalizer that the controller apparently used to optimize performance. The goodness of the approximation was judged visually. Table 5 presents the parameters of the transfer functions and shows also the gain-crossover frequency, ω_c.

TABLE 5

Effect of Display Separation on the Analytic Approximations to The Average Human Controller Describing Functions

	Display Separation					
	1-axis Tracking			2-axis Tracking		
	0°	30°	56°	0.8°	30°	56°
K_h (dB)	2	-5	-9	-1	-1	-6
ω_1 (rad/sec)	4	—	—	4	4	—
ω_2 (rad/sec)	10	—	—	8	8	—
τ (sec)	.12	.20	.30	.15	.15	.20
ω_c (rad/sec)	5.4	4.5	3.0	5.0	4.6	4.3

Display separation affected the describing functions in a number of ways. From the point of view of system performance, the most important effect was a decrease in K_h, which was essentially the amplitude ratio in the octave below the input cutoff frequency.* As the separation was increased from near 0° to 56°, the 1-axis K_h decreased by about 10 dB and the 2-axis K_h decreased by about 5 dB. The 1-axis effective time delay increased from 0.12 to 0.3 sec, whereas the 2-axis time delay varied only from 0.15 to 0.2 sec.

When tracking one axis foveally, the subjects generated an average lag term of $\omega_1=4$ rad/sec and a lead term of $\omega_2=10$ rad/sec. A lag frequency of 4 rad/sec was also generated for 2-axis tracking when the display separations were 0.8° and 30°, and the corresponding lead frequency was 8 rad/sec. No lead or lag terms were generated for either 2-axis or 1-axis peripheral tracking for the 56° display separation.

As the display separation was increased from minimum to maximum, the 1-axis gain-crossover frequency decreased from about 5.4 to 3.0 rad/sec, and the 2-axis ω_c decreased from about 5.0 to 4.3 rad/sec. Because the controller varied the shape as well as the gain of his describing function, variations in ω_c were less than the simple gain-crossover model of equation (1) would predict on the basis of changes in low-frequency gain; ω_c was thus only a partial indication of system performance.

---

* Since about 85% of the stick power is contained in this octave, the portion of mean-squared tracking error that is linearly correlated with the input signal will be largely determined by the amplitude ratios in this octave.

The describing functions have been replotted in Figure 12 so that the 1-axis foveal, 2-axis, and 1-axis peripheral DF appear together for each display separation. For separations of 30^{o} and 56^{o}, the 1-axis peripheral DF revealed a lower K_h, a flatter amplitude ratio curve, and a greater effective time delay than the 1-axis foveal DF. The 2-axis amplitude ratio and phase-shift curves fell between the corresponding 1-axis foveal and peripheral curves. When the separation was 0.8^{o}, the 1-axis foveal and 2-axis describing functions differed primarily in K_h.

The stick remnant power increased with increasing separation for both peripheral and 2-axis conditions (Table 4).* The peripheral remnant was greater than the 1-axis foveal remnant for separations of 30^{o} and 56^{o}, and the 2-axis remnant fell between the two. Changes in remnant error power generally paralled changes in remnant stick power.

(d) Eye Movements

The mean observation time, averaged over the L and R axes, was little effected by display separation (Table 4). The observation time increased from 1.2 to 1.3 seconds as the separation was increased from 30^{o} to 56^{o}.

The subjects spent about 60% of the time attending foveally to the R axis, although the total 2-axis MSE was about equally divided between the axes (Table A7). The differential allocation of attention may have been partly a result of task differences. Despite our best efforts to provide a homogeneous tracking environment, the R-axis NMSE

---

* Remnants for individual subjects are shown in Table A6.

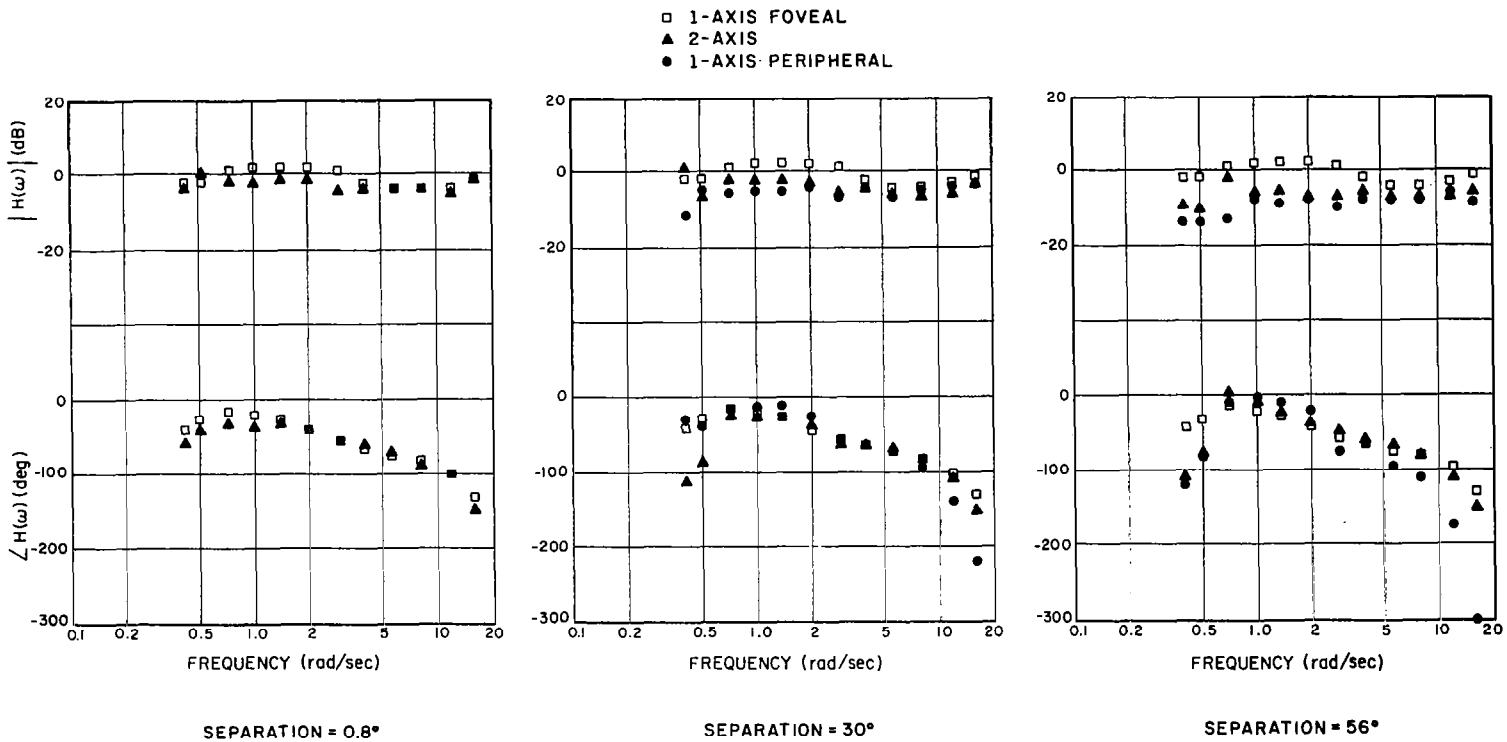

Fig. 12 Comparison of 1-axis Foveal, 1-axis Peripheral, and 2-axis Average Human Controller Describing Functions for Three Display Separations

Controlled elements: K/s
Input bandwidths: 2 rad/sec
Subjects: four

0 dB = 10^5 dynes/cm

was about 25% greater than the L-axis score in the 1-axis foveal situation and the R-axis peripheral NMSE was about 30% greater than the corresponding L-axis measurement.* The subjects may have had to devote more foveal attention to the R axis in order to achieve a balanced 2-axis MSE performance.

Probability density functions of observation time were computed for each subject for display separations of 30° and 56°; these functions were computed separately for the left and right axes. Table 6a gives the mean, the standard deviation (σ), and the σ/mean ratio for each density function.

Table 6b which gives the mean σ, and σ/mean ratio for the parameters of Table 6a, shows that the standard deviation of the probability density function was on the average 0.43 sec, or 33% of the mean observation time. The standard deviation of the density function, normalized with respect to mean observation time,(i.e., the SD/Mean ratio) was a less variable measure than the unnormalized standard deviation. The σ/mean ratios for these parameters were 0.21 and 0.37 respectively.

Figure 13 shows the average normalized probability density functions for display separations of 30° and 56°. Each curve is the average of six density functions--one per subject per axis--which were normalized with respect to the corresponding mean observation

* NMSE difference of 25% represents a difference in the human controller's gain of less than 1 dB. Thus, an observed L-R NMSE difference of this magnitude does not conflict with our earlier statement that there was no essential difference between the L and R DF's.

TABLE 6

Means and Standard Deviations of Observation Times
For Experiment 1

a. Means and Standard Deviations of the Probability Density Functions

Subject	Display Separation	Axis	Mean (sec)	σ (sec)	σ/Mean
JF	30°	L	0.8	.26	.32
		R	1.2	.36	.30
	60°	L	0.9	.18	.20
		R	1.3	.46	.35
DM	30°	L	1.1	.44	.40
		R	1.4	.64	.46
	60°	L	1.4	.39	.28
		R	1.8	.50	.28
PM	30°	L	1.1	.34	.31
		R	2.0	.66	.33
	60°	L	1.0	.30	.30
		R	1.6	.67	.42

b. Means and Standard Deviations of The Parameters of The Probability Density Functions.

Parameter	Mean	σ	σ/Mean
Mean Observation Time	1.3	.36	.28
SD of the Observation Time	.43	.16	.37
SD/Mean Ratio	.33	.070	.21

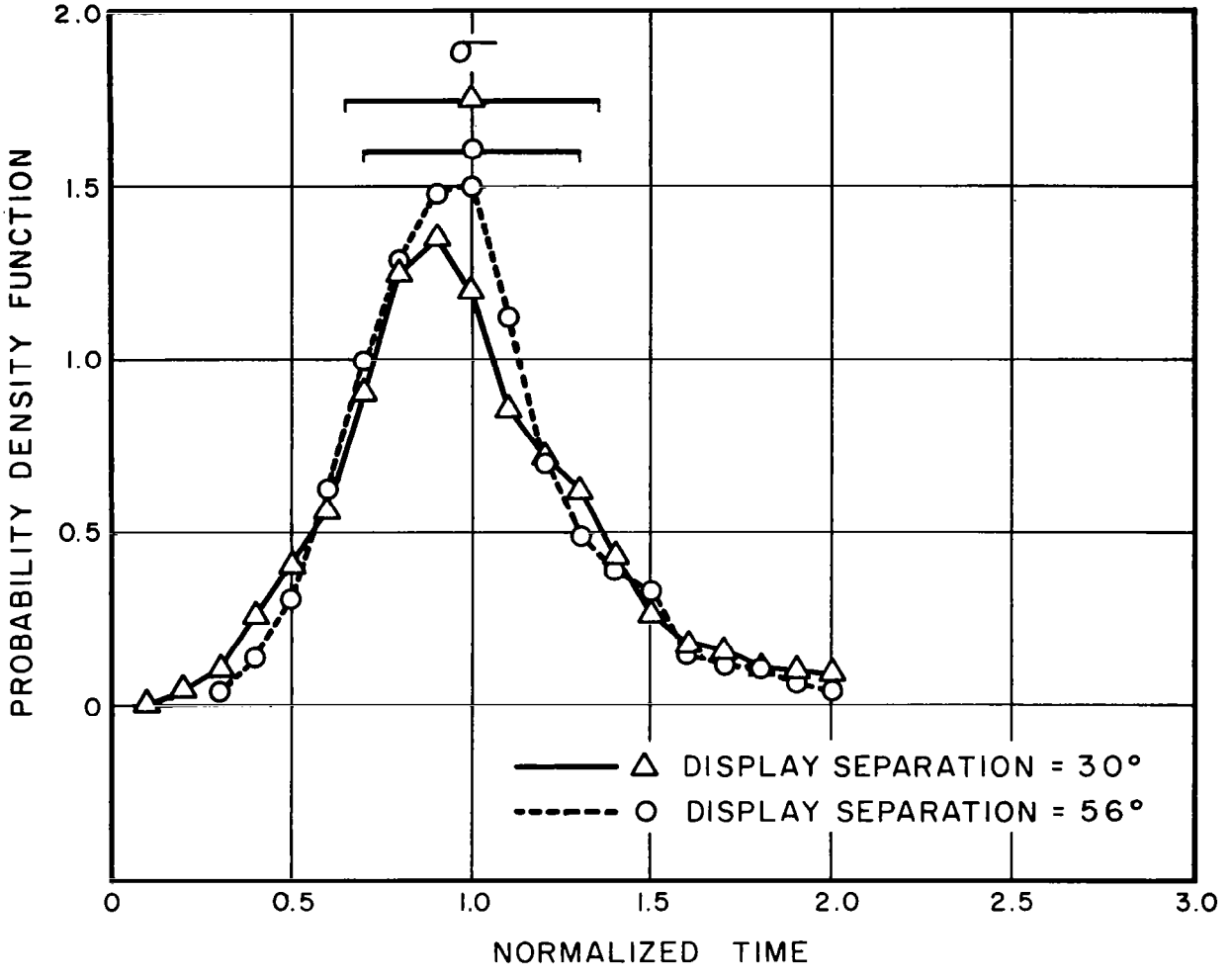

Fig. 13 Effect of Display Separation on The Normalized Probability Density Functions of The Observation Time

Controlled-elements: K/s
Input bandwidths: 2 rad/sec
Subjects: JF, DM, PM
0 dB = 10^5 dynes/cm

times. The standard deviations of the average normalized density functions were 0.34 and 0.30, respectively, for the 30° and 56° separations. The similarity of the two curves indicates that the visual scanning strategy was little affected by the magnitude of the display separation.

(e) Experimental Variability

Standard deviations of the NMSE, fractional remnant stick power mean observation time, and average low-frequency human controller gain were computed (for this experiment only) to indicate inter-subject variability. These are shown in Table 7. The average low-frequency gain was defined as the average of the amplitude ratio measurements obtained at 1.0, 1.4, and 2.0 rad/sec (the octave critical to system performance). Standard deviations of the subject means were computed and average L-R measurements were taken when possible.

The display separation had inconsistent effects on both the standard deviation and on the ratio of the standard deviation to the grand mean. The standard deviations of the low-frequency gains were between 1 and 3 dB, which indicates a relative uniformity of control behavior among subjects. Since the difference between the 1-axis foveal and 1-axis peripheral NMSE scores were on the order of ten times the corresponding standard deviations, these differences were statistically significant.

(f) Summary

Peripheral and 2-axis NMSE scores and fractional remnant powers increased as the display separation was increased. Although tracking performance was degraded simply by the requirement to track two non-integrated axes simultaneously, most of the difference between 2-axis and 1-axis foveal performance was attributed directly to

TABLE 7

Effect of Display Separation on the Variability of the Results
Mean-squared Error, Remnant, Mean Observation Time, and
Low-frequency Gain

		Display Separation					
		1-axis Tracking			2-axis Tracking		
		0°	30°	56°	0.8°	30°	56°
NMSE	Mean	.050	.36	.80	.073	.19	.42
	SD	.011	.013	.066	.017	.0063	.057
	SD/Mean	.23	.038	.083	.24	.034	.14
Fractional Remnant Stick Power	Mean	.17	.48	.65	.19	.40	.54
	SD	.028	.11	.070	.022	.074	.12
	SD/Mean	.16	.22	.11	.11	.19	.23
Mean Observation Time (sec)	Mean	-	-	-	-	1.2	1.3
	SD	-	-	-	-	.28	.24
Avg. Low-frequency Gain (dB)	Mean	1.8	-4.9	-8.4	-0.8	-2.3	-5.7
	SD	2.7	2.0	2.3	1.7	1.5	1.2

Sample Size:

4 subject means for the 1-axis foveal (0°) measurements

3 subject means for the 1-axis peripheral (30° and 56°) measurements

4 subject means for the 2-axis measurements

visual scanning. The most important change in the human controller's describing function was a progressive decrease of the low-frequency gain with increasing separation. There was no appreciable change in mean observation time.

2. Effects of Input Bandwidth

In this experiment we investigated the effects of input bandwidths of 0.5, 1, and 2 rad/sec on 1-axis-2-axis and foveal-peripheral differences in tracking performance.

(a) NMSE Scores

The average NMSE scores are summarized in Table 8, and the performances of the individual subjects are in Table A8. The 1-axis foveal, the 1-axis peripheral, and the 2-axis NMSE scores all increased with increasing bandwidth, as expected. The $\overline{NMSE_2/NMSE_f}$ ratio was about the same for the lowest two bandwidths (2.3 on the average) and increased to 3.6 when the bandwidth was 2 rad/sec. The $\overline{NMSE_p/NMSE_f}$ ratios showed a similar behavior and were from 1.5 to 2 times as great as the corresponding $\overline{NMSE_2/NMSE_f}$ ratios. Analyses of variance (Table A9) showed that the differences between the 2-axis and 1-axis peripheral scores were significant at the .001 level for all bandwidth-axis conditions. There were no significant number-subject interactions.

The R and L tasks were well balanced in that the average 1-axis foveal NMSE scores on the two axes differed by less than 10% for all bandwidth conditions (Table A8). The R-axis peripheral scores, however, were consistently about 30% greater than the L-axis scores, even though the display intensities and other visual stimuli were balanced. We did not investigate the source of this L-R performance difference, since it was not central to our experimental study.

TABLE 8

Effect of Input Bandwidth on Mean-squared Error, Remnant, and Mean Observation Time

		Input Bandwidth (rad/sec)		
		0.5	1.0	2.0
Normalized Mean-squared Errors	$NMSE_f$	.011	.020	.051
	$NMSE_p$	.037	.075	.36
	$NMSE_2$	.024	.045	.18
NMSE Ratios	$\overline{NMSE_2/NMSE_f}$	2.2	2.4	3.6
	$\overline{NMSE_p/NMSE_f}$	3.4	4.0	7.4
Fractional Remnant Stick Power	1-axis foveal	.16	.16	.17
	1-axis peripheral	.54	.44	.53
	2-axis	.34	.33	.34
Fractional Remnant Error Power	1-axis foveal	.20	.23	.27
	1-axis peripheral	.69	.67	.76
	2-axis	.46	.51	.48
Mean Observation Time	(seconds)	1.4	1.3	1.4

Controlled-element Dynamics: K/s

Display Separation: 30°

Subjects: JF, DM, PM

(b) Describing Functions and Remnant

The 1-axis foveal, 1-axis peripheral, and 2-axis human controller describing functions are shown in Figure 14 as a function of input bandwidth. The parameters of the approximate transfer functions are given in Table 9.

TABLE 9

Effect Of Input Bandwidth On The Analytic Approximations To The Average Human Controller Describing Functions

	Input Bandwidth (rad/sec)								
	1-axis Foveal			1-axis Periph.			2-axis		
	0.5	1.0	2.0	0.5	1.0	2.0	0.5	1.0	2.0
K_h (dB)	3	3	3	-3	0	-5	-1	1	-2
ω_1 (rad/sec)	.5	1	3	.5	1	---	.5	1	2
ω_2 (rad/sec)	1.5	3	10	1	2	---	1	3	3
τ (sec)	.15	0.15	0.12	.20	.20	.20	.20	.15	.15

The subjects adopted a similar strategy for all three 1-axis foveal tasks: the lag frequency (ω_1) was positioned near the input cutoff frequency, and the lead frequency (ω_2) was about three times greater than ω_1. K_h and τ were essentially invariant with bandwidth for the foveal task.

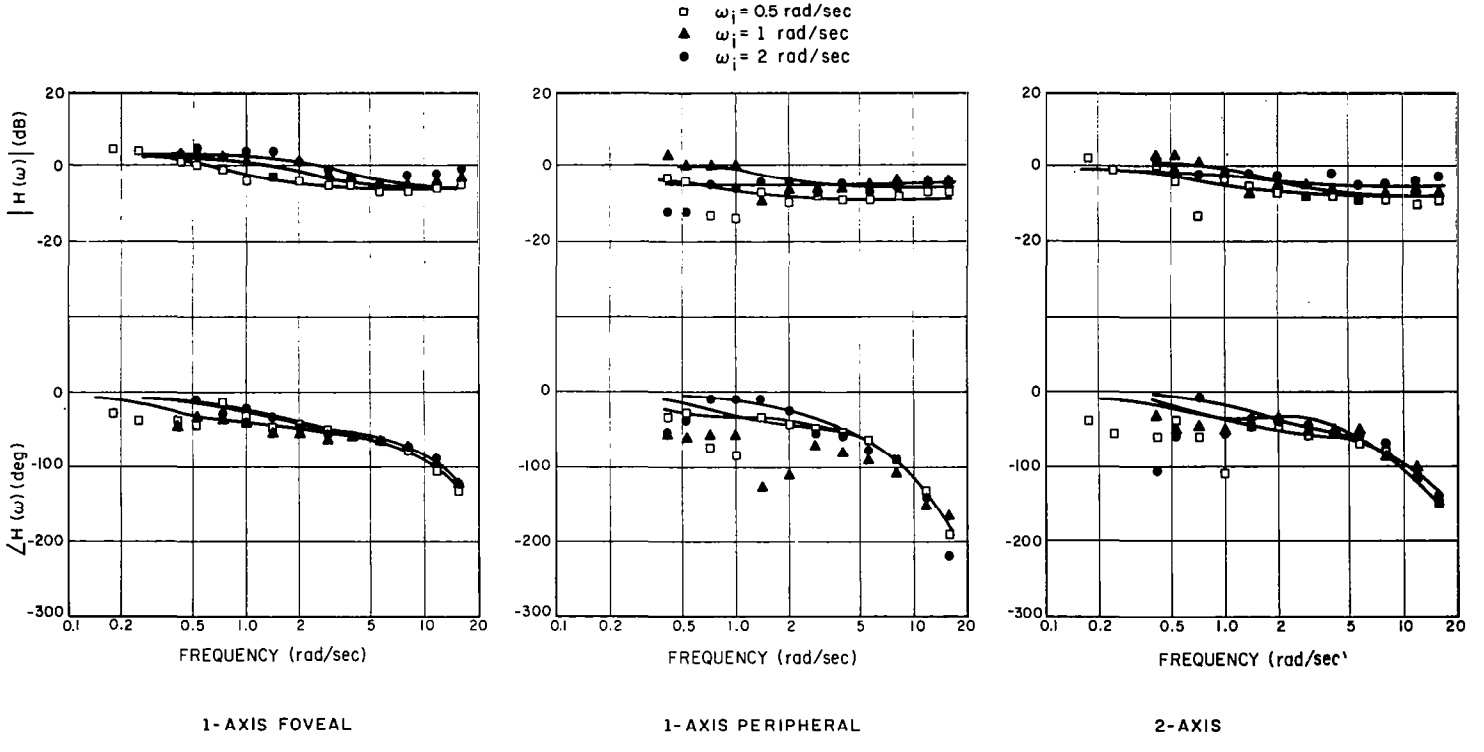

Fig. 14 Effect of Input Bandwidth on Average Human Controller Describing Functions

Controlled elements: K/s
Display Separation: 30 degrees
Subjects: three
0 dB = 10^5 dynes/cm

The 1-axis peripheral DF revealed an inconsistent bandwidth effect. K_h increased about 3 dB as the bandwidth was increased from 0.5 to 1 rad/sec and then decreased by about 5 dB as the bandwidth was further increased to 2 rad/sec. The slight lag-lead behavior observed for the slower inputs disappeared for the 2 rad/sec input.

The 2-axis DF's were less affected by bandwidth variations than the peripheral measurements. K_h ranged from 2 dB to 1 dB, the time delay ranged from 0.2 to 0.15 sec.

Figure 15 presents the 1-axis foveal, 1-axis peripheral, and 2-axis DF's for each bandwidth. The DF differences for all three bandwidth conditions show the same trend that we found in Experiment 1: (1) the average 1-axis peripheral K_h is lower than the 1-axis foveal K_h, (2) the 2-axis K_h falls between the two 1-axis K_h's and (3) the effective time delay appears to increase as the task proceeds from 1-axis foveal to 2-axis to 1-axis peripheral.

Average remnant data are presented in Table 8, and Table A10 contains the data for each subject. Bandwidth had no consistent effect on fractional remnant power.

(c) Eye Movements

Bandwidth had no consistent effect on mean observation times, which ranged from 1.3 to 1.4 sec (Table 8). The fact that the subjects consistently devoted about 58% of their foveal attention to the R axis while achieving a nearly even distribution of the 2-axis NMSE (Table A11) indicates that the R-axis task was the more difficult in the 2-axis situation.

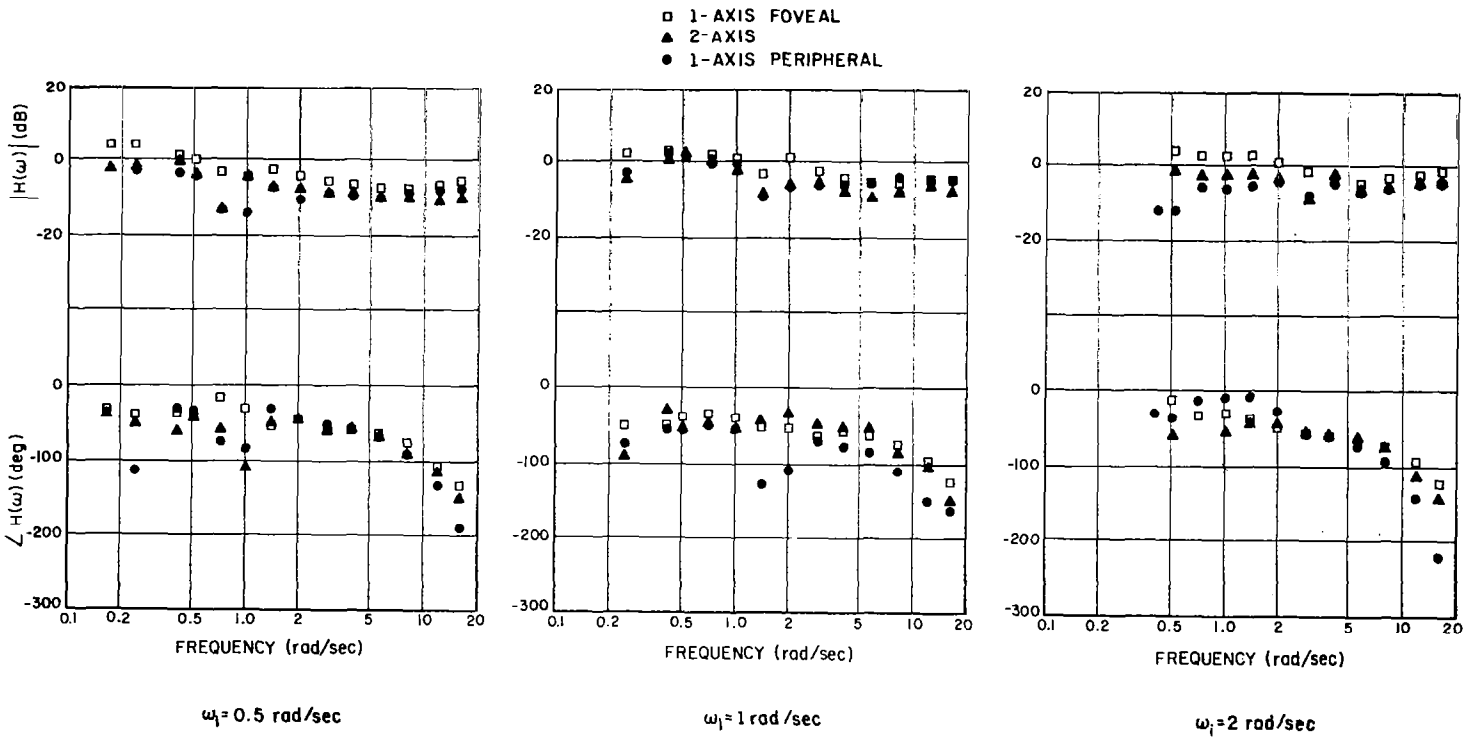

Fig. 15 Comparison of 1-axis Foveal, 1-axis Peripheral, and 2-axis Average Human Controller Describing Functions for Three Input Bandwidths

Controlled elements: K/s
Display Separation: 30 degrees
Subjects: three

0 dB = 10^5 dynes/cm

(d) Summary

Although the $\overline{NMSE_2/NMSE_f}$ and $\overline{NMSE_p/NMSE_f}$ ratios were relatively unchanged as the input bandwidth was increased from 0.5 to 1 rad/sec, the ratios increased by 50% or more as the bandwidth was further increased to 2 rad/sec. Small and inconsistent changes occurred in low-frequency gain. Neither mean observation time nor fractional remnant power was a function of bandwidth.

3. Effects of Axis Differences

In this experiment we investigated the effects of axis differences on the relationship between 1-axis foveal and 2-axis performance and on the allocation of foveal attention between the two axes.

(a) NMSE Scores

As a convenient way of presenting the results, we shall treat one axis (Axis A) as an axis of constant input bandwidth, and the other axis (Axis B) as the axis of variable bandwidth. The mean-squared inputs (MSI) on both axes are treated as variables. (Details on the experimental procedure are given in Chapter III.)

Table 10a presents the average results obtained on the "low-bandwidth axis"--the axis on which the input bandwidth is considered fixed at 0.5 rad/sec. The results are organized so that the 2-axis mean-squared error score on Axis B, relative to the score on Axis A, increases as one proceeds across a row of data. The first column of data corresponds to the homogeneous tracking situation with ω_i=0.5 rad/sec and the same MSI on both axes. The second column corresponds to the different-bandwidth condition in which ω_i was 2 rad/sec on Axis B and the MSI were adjusted to provide equal 1-axis foveal mean-squared errors on the two axes. The third column corresponds to the different-bandwidth condition in which the MSI were identical on both axes. This condition resulted in a much greater 1-axis MSE score on Axis B than on Axis A.

TABLE 10

Effect of Axis Differences on Mean-squared Error, Foveal Attention, Remnant, and Mean Observation Time

a. Axis A = Low-bandwidth Axis (ω_i = 0.5 rad/sec)

		Conditions on Axis B		
		Same BW Same MSI	Diff. BW Diff. MSI	Diff. BW Same MSI
Normalized MS Error	$NMSE_f$	.011	.011	.010
	$NMSE_2$	.024	.028	.083
NMSE Ratio	$NMSE_2/NMSE_f$	2.2	2.6	8.2
Fractional Allocation	Total 2-Axes MS Error	.50	.45	.39
	Foveal Attention	.50	.43	.37
Fract. Remnant Stick Power	1-Axis Foveal	.16	---	.21
	2-Axes	.34	.41	.59
Fract. Remnant Error Power	1-Axis Foveal	.20	---	.29
	2-Axes	.46	.52	.63
Mean Observation Time (seconds)		1.4	1.3	1.2

b. Axis A = High-bandwidth Axis (ω_i = 2.0 rad/sec)

		Conditions on Axis B		
		Diff. BW Same MSI	Diff. BW Diff. MSI	Same BW Same MSI
Normalized MS Error	$NMSE_f$	.047	.046	.051
	$NMSE_2$	.13	.14	.18
NMSE Ratio	$NMSE_2/NMSE_f$	2.8	3.0	3.6
Fractional Allocation	Total 2-Axes MS Error	.61	.55	.50
	Foveal Attention	.63	.57	.50
Fract. Remnant Stick Power	1-Axis Foveal	.15	----	.17
	2-Axis	.30	.35	.34
Fract. Remnant Error Power	1-Axis Foveal	.20	----	.27
	2-Axis	.44	.46	.48
Mean Observation Time (seconds)		2.0	1.7	1.4

Controlled-element Dynamics: K/s
Display Separation: 30°
Subjects: JF, DM, PM

Average results for the "high-bandwidth axis" (ω_i=2.0 rad/sec) are presented in Table 10b. The results are similarly organized in that the relative difficulty (i.e., the MSE score) of the 2-axis task on Axis B increases as one procedes across a row of data.

All mean-squared error and eye movement results in Table 10 are based on equal contributions of data from the L and R axes. Remnant data are for R-axis tracking only. Mean-squared error data for individual subjects for the different-bandwidth conditions are given in Table A12.

The relative difficulty of the A- and B-axis tasks is reflected by the allocation of total mean-squared error. For example, the fraction of the total error appearing on the low-bandwidth axis decreased from 0.50 to 0.39 as the relative difficulty of the task on Axis B was increased.* Similarly, the fraction of total error appearing on the high-bandwidth axis decreased from 0.61 to 0.50 with increasing difficulty of the B-axis task.

Changes in the 2-axis $NMSE_2$ ran counter to changes in the fractional allocation of total error; the $\overline{NMSE_2/NMSE_f}$ ratio on Axis A increased as the relative difficulty of the task on Axis B increased. This trend was more pronounced on the low-bandwidth axis, on which the ratio ranged from 2.2 for the homogeneous control situation to 8.2 for the different-bandwidth, same MSI condition.

---

* Since measurements have been averaged over the L and R axes, half the foveal attention and half the total mean-squared error were, by definition, allocated to Axis A when the control conditions were the same for both axes.

Analyses of variance (Table A13) showed that the differences between the 1-axis foveal and 2-axis scores were significant at the .001 level for the high-and low-bandwidth axes in the two heterogeneous tracking conditions. There were no number-subject interactions.

The goal of providing equal 1-axis foveal tasks in the different-bandwidth, different MSI condition was reasonably well achieved: the high- and low-bandwidth 1-axis MSE's were within 10% of each other (Table A12). On the other hand, the tasks were not equal in the 2-axis situation, 55% of the total 2-axis error appeared on the high-bandwidth axis in this tracking situation (Table 10).

(b) Describing Functions and Remnant

Two-axis describing functions for Axis A are shown in Figure 16 as a function of conditions on Axis B; the approximate transfer-function parameters are given in Table 11. Important changes occurred only on the low-bandwidth axis. K_h decreased by about 8 dB and the lag-lead behavior disappeared as the difficulty of the B-axis task was increased. The lack of a measurable effect on the high-bandwidth DF was consistent with the small differences in the NMSE scores on that axis.

Similar effects of axis differences were seen on the fractional remnant measures.* As the relative difficulty of the B-axis task was varied between its minimum and maximum, the fractional remnant stick power increased by a factor of 1.8 and the remnant error power by 1.4 on the low-bandwidth axis (Table 10). There was little change in remnant on the high-bandwidth axis.

---

* Remnant data for individual subjects are given in Table A14.

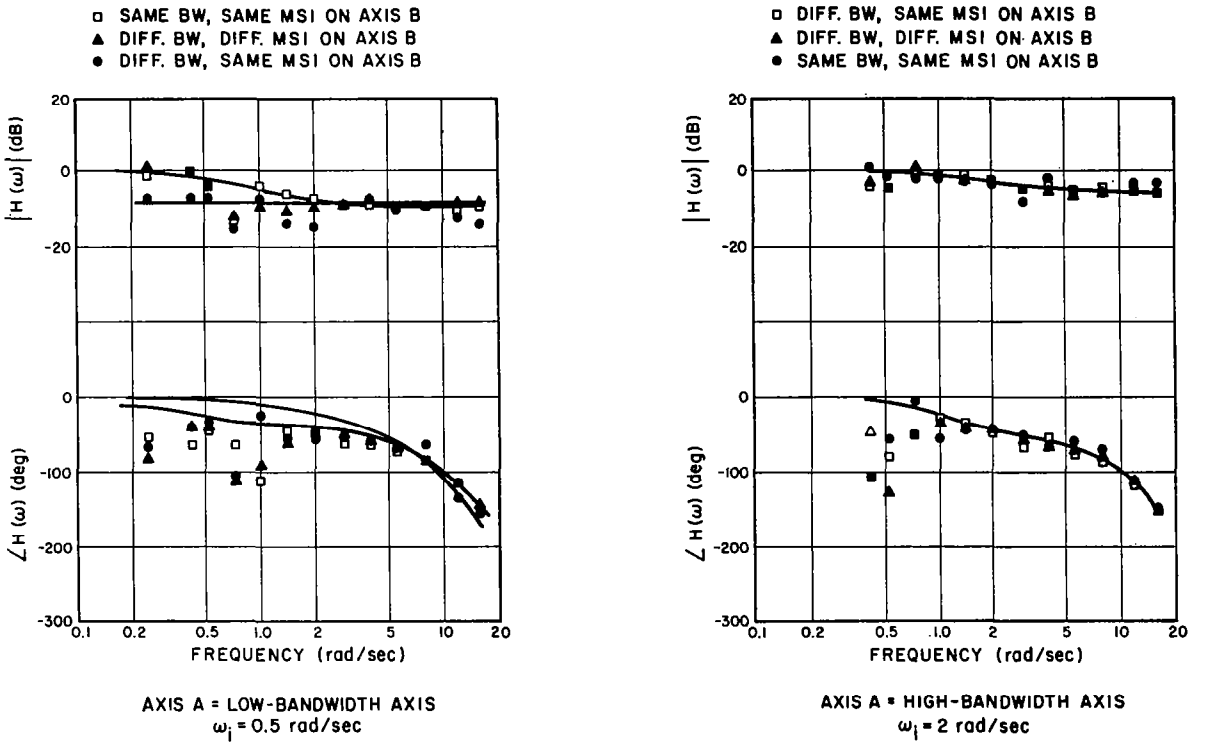

Fig. 16 Effect of Axis Differences on Average Human Controller Describing Functions

Controlled elements: K/s
Display separation: 30 degrees
Subjects: three

0 dB = 10^5 dynes/cm

TABLE 11

Effect of Axis Differences on The Analytic Approximations To The Average Human Controller Describing Functions

	Conditions on Axis B			
	Low-Bandwidth Axis			High-Bandwidth Axis
	Same BW Same MSI	Diff. BW Diff. MSI	Diff. BW Same MSI	All Conditions
K_h (dB)	0	0	-8	0
ω_1 (rad/sec)	.5	.5	--	1.5
ω_2 (rad/sec)	1.5	1.5	--	3
τ (sec)	.18	.18	.20	.18

(c) Eye Movements

The fraction of the subject's foveal attention allocated to Axis A, as well as the mean dwell time on Axis A, decreased as the relative difficulty of the task on Axis B increased (Table 10).* Furthermore, the division of foveal attention was on the average nearly equal to the division of the total MSE between the two axes for all control conditions.

---

* Table A15 contains eye-movement data for individual subjects.

(d) Summary

As the difficulty of the task on Axis B increased relative to the task on Axis A, an increasing fraction of foveal attention was devoted to Axis B; the NMSE score on Axis A was allowed to increase; and the mean observation time on Axis A decreased. The fraction of foveal attention devoted to either axis was approximately equal to the fraction of the total mean-squared error appearing on that axis. When Axis A contained the low-bandwidth task, the controller's low-frequency gain decreased and his remnant increased as the relative difficulty of the B-axis task was increased.

4. Effects of Controlled Element Dynamics

In this experiment we investigated the effects of controlled-element dynamics of K, K/s, and K/s^2 on the relations among 1-axis foveal, 1-axis peripheral, and 2-axis performance.

(a) NMSE Scores

Table 12 shows that both the $\overline{NMSE_2/NMSE_f}$ and $\overline{NMSE_p/NMSE_f}$ ratios decreased slightly as the complexity of the dynamics was increased from K to K/s, but increased by factors of 2.1 and 1.6, respectively, as the dynamics were changed to K/s^2. Computations based on the individual performances shown in Table A-16 reveal that the spread of the $\overline{NMSE_2/NMSE_f}$ ratio among subjects increased with the order of the dynamics from about 57% for dynamics of K to about 75% from the K/s^2 dynamics.

Table A-17 shows that the differences between the 1-axis foveal and 2-axis NMSE scores were significant at the .001 level for the L, R, and total-task measurements when the dynamics were

TABLE 12

Effect of Controlled-Element Dynamics
on Mean-Squared Error, Remnant, and
Mean Observation Time

		Controlled-Element Dynamics		
		K	K/s	K/s^2
Normalized Mean-Squared Errors	$NMSE_f$	.018	.020	.052
	$NMSE_p$	.085	.075	.34
	$NMSE_2$	.053	.045	.26
NMSE Ratios	$\overline{NMSE_2/NMSE_f}$	2.9	2.4	5.1
	$\overline{NMSE_p/NMSE_f}$	4.3	4.0	6.6
Fractional Remnant Stick Power	1-axis foveal	.032	.16	.45
	1-axis peripheral	.084	.44	.84
	2-axis	.055	.33	.80
Fractional Remnant Error Power	1-axis foveal	.28	.23	.46
	1-axis peripheral	.55	.67	.73
	2-axis	.44	.51	.69
Mean Observation Time (seconds)		1.4	1.3	1.2

Input Bandwidth: 1 rad/sec
Display Separation: 30°
Subjects: JF, DM, PM

K and K/s and that there were no number-subject interactions under those conditions. Significant subject-number interactions appeared for K/s^2 dynamics on the R-axis (.01) and total-task (.05) measurements. As a result, only the L-axis difference was significant at the .001 level. It should be noted that the 2-axis NMSE was greater than the 1-axis NMSE for all replications of the experiment with K/s^2 dynamics; the number-subject interaction arose because the magnitude of this difference vaied among the subjects.

(b) *Describing Functions and Remnant*

Figure 17 shows the 1-axis foveal, 1-axis peripheral, and 2-axis human controller describing functions for each of the controlled elements. The parameters of the approximate transfer functions are given in Table 13. The approximation to the controller's describing function for controlled-element dynamics of K is

$$H(j\omega) = K_h \frac{(1+j\frac{\omega}{\omega_2})}{(1+j\frac{\omega}{\omega})\ (1+j\frac{\omega}{\omega_1})}\ e^{-\tau s} \qquad (7)$$

and for controlled-element dynamics of K/s^2 is

$$H(j\omega) = j\omega K_h \frac{(1+j\frac{\omega}{\omega_2})}{(1+j\frac{\omega}{\omega_1})}\ e^{-\tau s} \qquad (8)$$

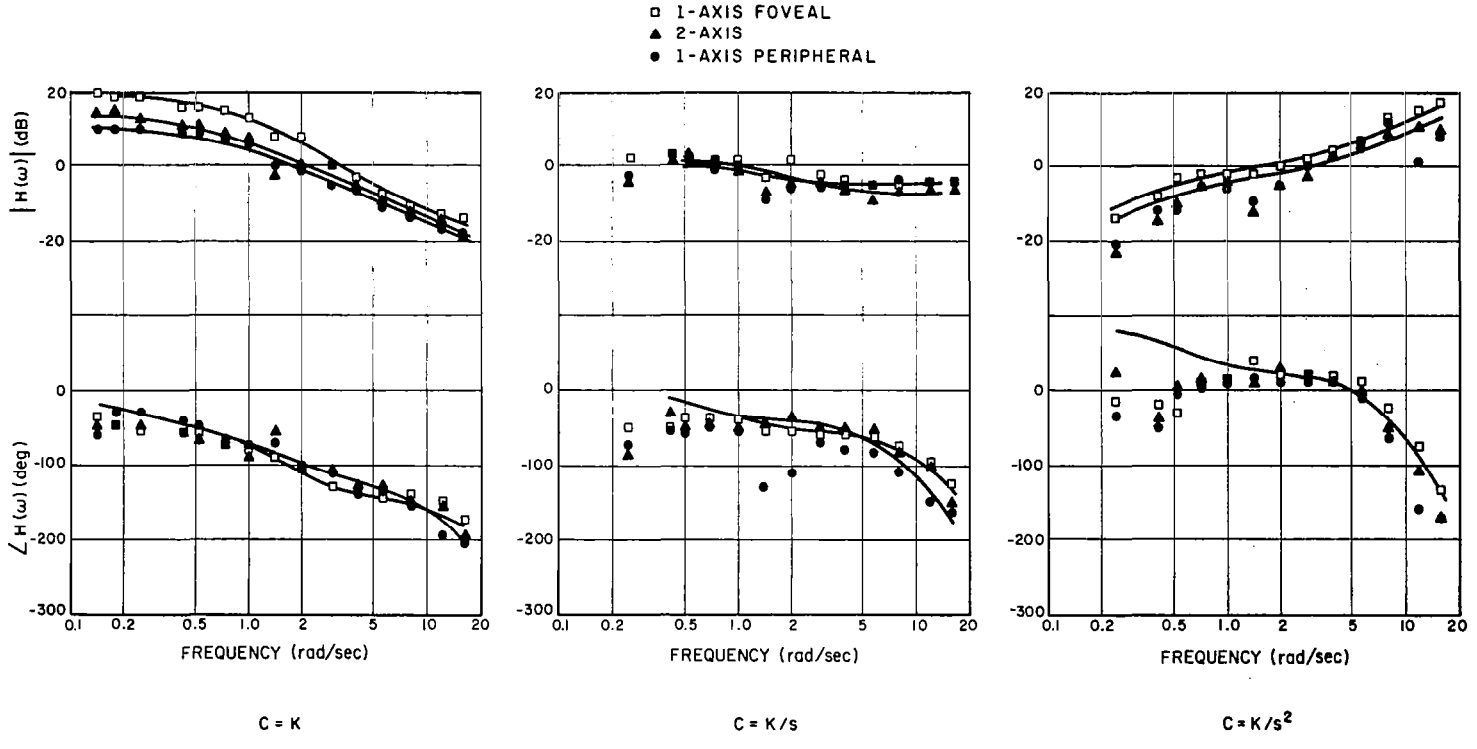

Fig. 17 Comparison of 1-axis Foveal, 1-axis Peripheral and 2-axis Average Human Controller Describing Functions for Three Controlled-element Dynamics

Input bandwidths: 1 rad/sec
Display separation: 30 degrees
Subjects: three

0 dB = 10^5 dynes/cm

TABLE 13

Effect of Mode of Tracking on the Analytic Approximations to the Average Human Controller Describing Functions for Controlled Dynamics of K, K/s, and K/s^2

	Mode of Tracking								
	K			K/s			K/s^2		
	F	P	2	F	P	2	F	P	2
K_h (dB)	19	10	14	3	0	1	1	-2	-2
ω_0 (rad/sec)	.5	.5	.4	-	-	-	-	-	-
ω_1 (rad/sec)	2	-	-	1	1	1	1	1	1
ω_2 (rad/sec)	4	-	-	3	2	3	3	3	3
τ (sec)	.10	.10	.12	.15	.20	.15	.25	.25	.25

Mode of Tracking

F = 1-axis foveal

P = 1-axis peripheral

2 = 2-axis

K_h was lower for 1-axis peripheral tracking than for 1-axis foveal tracking for all controlled-element dynamics. The greatest foveal-peripheral difference occurred with dynamics of K (9 dB), whereas the smallest (2 dB) occurred with K/s dynamics. The mid-frequency lag-lead characteristic evident in all 1-axis foveal describing functions disappeared for peripheral and 2-axis tracking when the dynamics were K. Variations of effective time delay with mode of tracking were less than 0.05 sec. The 2-axis amplitude-ratio and phase shift curves generally fell between the 1-axis foveal and 1-axis peripheral curves.

That the greatest decrease in controller gain should occur with K dynamics seems inconsistent with the observation that the greatest $\overline{NMSE_p/NMSE_f}$ and $\overline{NMSE_2/NMSE_f}$ ratios occurred with K/s^2 dynamics. The controller's gain-crossover frequency and phase margin, however, were greater for K dynamics, a given amount of gain decrease may therefore have had a more adverse effect on system performance when the dynamics were K/s^2 than when they were K.

Figure 18 shows the open-loop describing functions as a function of controlled-element dynamics. (The open-loop describing function is defined as the controller's describing function cascaded with the controlled-element transfer function.)

The gain-crossover frequency was nearly identical for K and K/s dynamics, and was about an octave less for K/s^2 dynamics. Phase margins were greater than 20 degrees when the dynamics were K and K/s, but were reduced to about 10 degrees for peripheral and 2-axis tracking when the dynamics were K/s^2.

The average fractional stick remnant power increased markedly with the order of dynamics (Table 12).* The 1-axis foveal remnant ranged from .032 for K dynamics to .45 for K/s^2 dynamics. The 2-axis remnant stick was about twice the 1-axis foveal remnant, and the peripheral remnant was somewhat greater. The fractional remnant error power also generally increased with the order of the dynamics, but the changes were less extreme.

---

* Remnant data for individual subjects are given in Table A18.

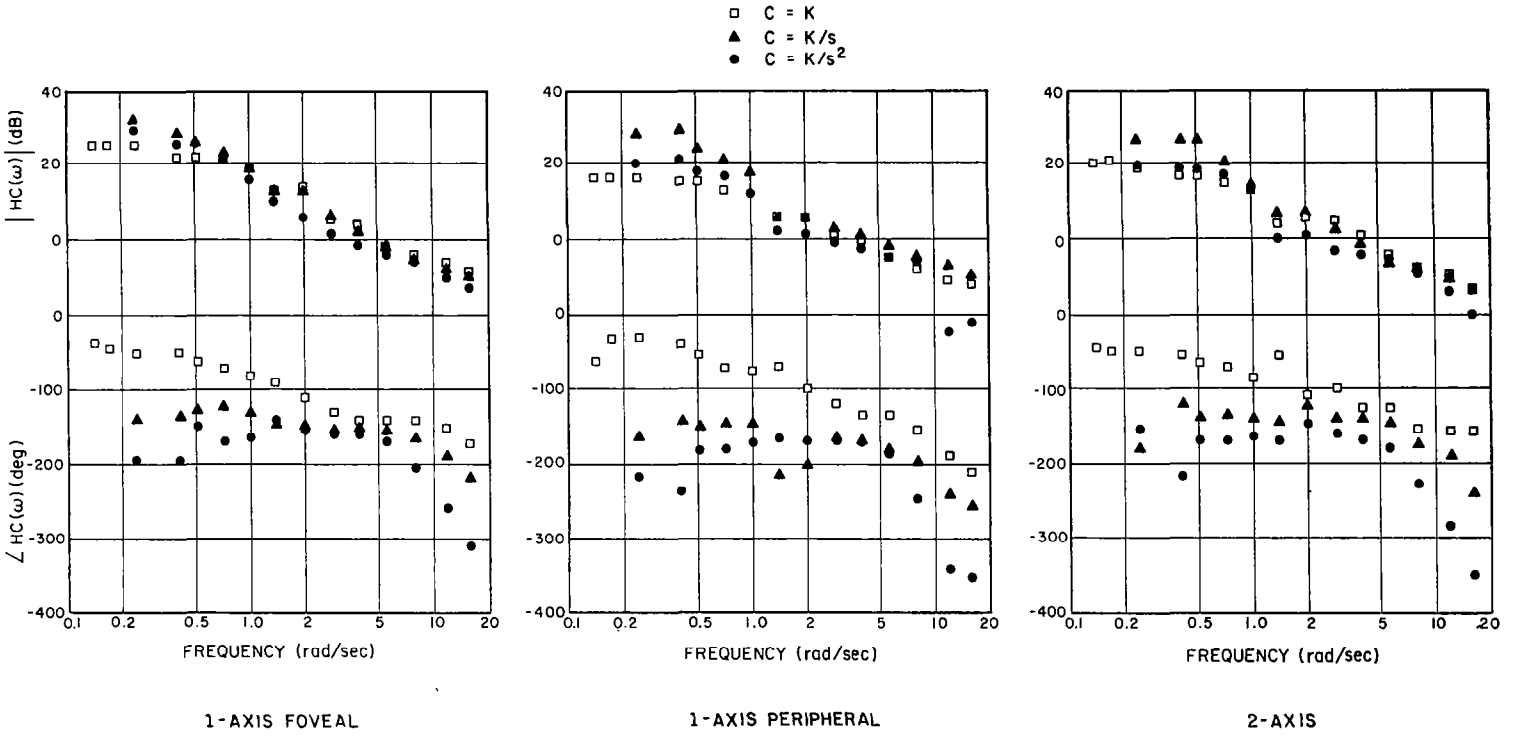

Fig. 18 Effect of Controlled-element Dynamics on Average Human Controller Describing Functions

Input bandwidths: 1 rad/sec
Display separation: 30 degrees
Subjects: three

0 dB = 10^5 dynes/cm

(c) Eye Movements

Mean observation times, shown in Table 12, decreased from 1.4 to 1.2 sec as the order of the dynamics was increased from K to K/s^2. This variation is insignificant, however, when compared to inter-subject variations. The mean observation time ranged from 0.6 sec for subject DM to 1.9 sec for subject PM when the dynamics were K/s^2, (Table A19). The observation time of 0.6 sec represented almost twice the scanning rate exhibited by any other subject under any condition (and twice the rate exhibited by DM under any other tracking condition). On the other hand, 1.9 sec was the longest observation time shown by any subject under homogeneous tracking conditions. The spread of mean observation times along subjects was considerably less for dynamics of K and K/s.

(d) Summary

The peripheral and 2-axis NMSE, relative to the 1-axis foveal NMSE, remained about the same for K and K/s dynamics, but increased by almost a factor of 2 when the dynamics were changed to K/s^2. A change in the mode of tracking effected the controller's describing function primarily through a change in low-frequency gain for all controlled-element dynamics. There were no consistent changes in the relation between 1-axis foveal, 1-axis peripheral, and 2-axis remnants. Mean observation times decreased slightly as the order of the dynamics was increased, and inter-subject variations were greatest when the dynamics were K/s^2.

5. Summary

The effects of display separation, input bandwidth, axis differences and controlled-element dynamics on 2-axis and peripheral tracking performance were investigated. The primary difference between the 1-axis foveal, 1-axis peripheral, and 2-axis human controller describing functions in all experiments was a difference in the controller's low-frequency gain. These gain differences were generally consistent with the corresponding NMSE differences. Other describing-function differences appeared to be of secondary importance with respect to system performance.

Two-axis and peripheral tracking performance was degraded as the display separation was increased: the NMSE increased, the fractional remnant power increased, and the controller's gain decreased. There was no appreciable effect on the mean observation time.

Bandwidth had a non-uniform effect on tracking performance. The 2-axis and 1-axis peripheral NMSE scores, relative to the 1-axis foveal NMSE score, remained roughly constant for bandwidths of .5 and 1 rad/sec and increased by more than 50% when the bandwidth was increased to 2 rad/sec. Mean observation times and fractional remnant powers were unaffected by bandwidth.

The order of the controlled-element dynamics produced a similar non-uniform effect on the controller's behavior. The 2-axis and peripheral NMSE scores, relative to the 1-axis foveal NMSE score, remained about the same for K and K/s dynamics and then increased by almost a factor of 2 when the dynamics became K/s^2. There were no consistent changes in the relation between 1-axis and 2-axis remnant, and there was only a slight decrease

in mean observation time as the order of the dynamics was increased. Inter-subject variations increased with the order of the dynamics.

The subject's allocation of foveal attention was affected by the relative task difficulties. As the mean squared error score of the task on Axis B was increased, relative to that on Axis A, the subject devoted less of his foveal attention to Axis A, lowered his effective gain on Axis A, and allowed the NMSE on that axis to increase. The fraction of foveal attention devoted to an axis was on the average equal to the fraction of the total 2-axis mean squared error appearing on that axis.

CHAPTER VI
DISCUSSION

A. General Discussion of The Results

1. Horizontal-Vertical Differences

The greater 2-axis NMSE scores observed in the horizontal axis in the preliminary experiments may have resulted from a higher threshold to peripheral motion on that axis. McColgin (Ref. 15) found that the threshold to vertical motions was lower than the threshold to horizontal motions for motions about the horizontal axis. Furthermore, the subjects claimed that the vertical peripheral motions were more attention-getting than the horizontal peripheral motions. (We did not attempt to measure thresholds or other nonlinearities in this set of experiments.)

2. Remnant

Velocity threshold effects may have been a principal cause of the large remnant observed in the controller's output when a single axis was tracked peripherally. The subjects claimed that they were unable to perceive the error dot when it was moving too slowly.* They claimed further that the stationary reference circle could not be seen at all peripherally.

A threshold of this nature could result in an effective dead zone of variable location. The resultant nonlinear and time-varying control strategy would be revealed by our measurement technique as increased remnant.

---

* During the initial phases of peripheral training, the subjects often "dithered" the error dot when it was otherwise moving slowly so that they could determine its position. After they became more proficient in the task, they assumed that a dot that they couldn't see was within the reference circle.

We can identify two sources of the 2-axis remnant if we assume that the operator switches between foveal and peripheral strategies on a given axis when tracking two axes simultaneously. First, one would expect the 2-axis remnant to be a weighted sum of the remnants associated with the 1-axis foveal and peripheral tasks. Second, because our analysis procedure considers as remnant all signal power not accounted for by a time-invariant linear strategy, remnant will be measured even if the individual strategies are remnant-free.

3. Mean Observation Times

The mean observation times that we observed were generally a factor of 3 to 5 greater than those observed by Fitts et al (Ref. 22) in studies of simulated flight situations. This discrepancy may have stemmed directly from the differing nature of the monitoring tasks in the two studies.

In our experiments, there was only one display pertinent to each axis. Thus, it was necessary for the subject to obtain as much information as possible from each display in order to achieve good system performance. In the flight situation, however, a multiplicity of instruments supplied information for the various axes of control. Shorter observation times may have been required in that situation because (1) the correlations between instrument readings may have allowed some prediction of the readings, and (2) task performance was less critically dependent on the information obtained from any one instrument.

Senders (Ref. 12) measured observation times much smaller than ours in his studies of the human monitor, even when the signals on the various instruments were unrelated. We suspect

that this difference arose because our subjects were required to track the signals, whereas Senders' subjects were required only to monitor the signals with no means of control.

4. Relation Between Gain, System Performance, and Attention

Experiment 3 showed that the gain on a given axis tended to decrease as the controller was required to devote a decreasing fraction of his foveal attention to that axis. In addition, we found that the fraction of attention devoted to an axis was on the average equal to the fraction of the total mean-squared error appearing there. These observations suggest that (a) controller's gain, relative to the gain achieved in 1-axis tracking, is a measure of attention, and (b) attention is a measure of the relative difficulty of a component task and thus is related to the "workload" imposed by a task. These notions are consistent with the models of the human controller developed in the following section of this chapter.

5. A Model for Peripheral Tracking Behavior

We have found that effective control is possible when a single error variable is displayed well into the periphery of the visual field. The single-axis models of the human controller, such as those presented by McRuer et al (Ref. 3), ought therefore to be extended to apply to the 1-axis peripheral tracking situation.

The simplest of these models, given in equation (1) of this report, requires only a single descriptor of the human controller--the effective time delay τ_e. Knowledge of τ_e and of the parameters of the tracking situation enable one to predict the

gain-crossover frequency, the controller's describing function, and the mean-squared error performance with reasonable accuracy in many tracking situations (Ref. 3). In situations in which the controller's nonlinearities or time-variations are significant, some description of the controller's remnant should be given.

Figure 19 shows that both the effective time delay and the stick remnant are approximately linear functions of the display separation for the 1-axis peripheral tracking conditions investigated by us in Experiment 1. The remnant measure shown is the ratio of remnant stick power to input-correlated stick power and was derived from the fractional remnant powers given in Table 4. The effective time delays are from Table 5.

Since the controller's ability to obtain peripheral information is highly dependent on the characteristics of the information source and on the structure of the visual field, we should be cautious about generalizing these results. Further experimentation is necessary to determine the effects of experimental parameters such as mean-squared input, bandwidth, plant dynamics, display brightness, and complexity of the visual field on the relationships shown in Figure 19. Should these relationships remain approximately linear, and should they vary in a predictable way with variations in the tracking situation, then relatively straightforward modifications to the existing single-axis models of the human controller should allow good predictions of peripheral tracking performance.

6. Performance Criteria

The performance measure that we used--total mean-squared error--was not sensitive to scanning behavior in our 2-axis experiments. While training with homogeneous tracking conditions,

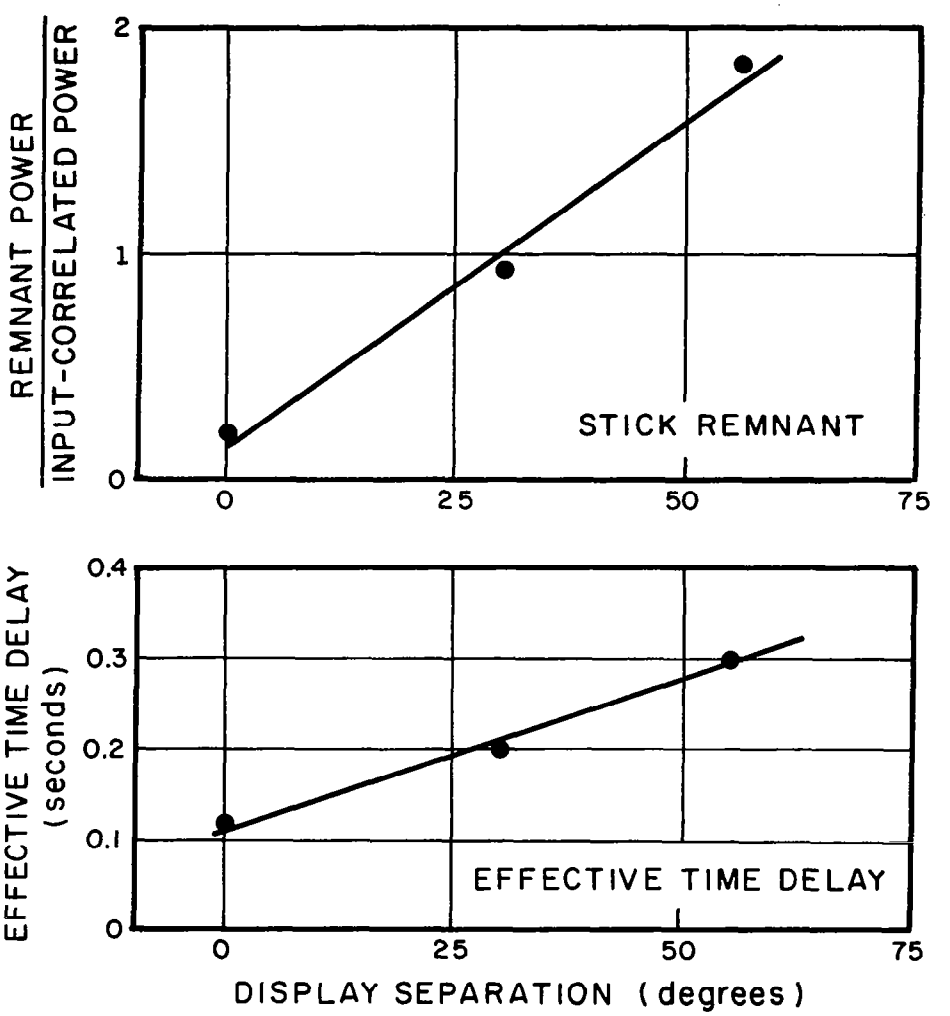

Fig. 19 Effect of Display Separation on Stick Remnant and Effective Time Delay for 1-axis Peripheral Tracking

Controlled elements: K/s
Input bandwidths: 2 rad/sec
Subjects: three

the subjects occasionally attended preferentially to one axis without appreciably degrading their total MSE. That is, they were able to some extent to trade errors on one axis for errors on the other.

Although the mean-squared error measure provides a useful indication of system performance from an engineering standpoint, it is apparently not a good criterion to employ experimentally if one wishes to control the scanning behavior of the human controller. Performance criteria that yield a sharper relation between error and score--such as time-off-target--may provide better experimental control.

B. A Simple Model For Tracking With Separated Displays

It appears from our experimental results that multiaxis models for the human controller can be constructed from a simple combination of single-axis models of the type presented by McRuer et al (Ref. 3). The art of modelling multiaxis control situations will be greatly facilitated if this proves to be true in general. One will then be able to predict system performance from the system parameters by applying a set of straightforward combinatorial rules to the existing human controller models.

1. Properties of The Model

A simple switching model of the human controller predicts with reasonable accuracy the effects of visual scanning on system performance. The key assumption of this model is that the human controller acts as a two-channel processor of information: one channel processes information obtained foveally while the other simultaneously processes information obtained peripherally. There is assumed to be no coupling, or interference, between channels.

These assumptions lead to the model shown in Figure 20, in which the human controller's strategy on each axis of a two-axis task can be represented by two dynamic elements whose outputs are added and whose inputs are switched. One of these elements, $H_{fa}(\omega)$, is assumed to be equal to the describing function generated when the subject tracks axis A alone. The other, $H_{pa}(\omega)$, is equal to the describing function appropriate to single-axis peripheral tracking. A second pair of elements describes the controller's strategy on axis B. Remnant terms are associated with all four describing functions. Switching on the two axes is coupled so that $H_{fa}(\omega)$ is applied simultaneously with $H_{pa}(\omega)$. This model does not include sample-and-hold mechanisms. When signal e_a is applied to element H_{fa}, for example, the signal applied to element H_{pa} is assumed to be zero.

A physical representation of the model was constructed on the analog computer so that the model's predictive value could be tested. Experiments were performed to compare the 2-axis describing functions and mean-squared error performance of the model with those of the human controllers.

Tracking with K/s dynamics was simulated. The controller's foveal and peripheral describing functions were both simulated by filters of the form $H(s)=K\ e^{-0.2s}$. The "foveal gain" was adjusted to yield an NMSE as close as possible to that achieved by the human controller when tracking a single axis.* The "peripheral gain" was adjusted to yield an NMSE typical of

---

* The human controller describing functions that we measured contained a lag-lead characteristic that enabled the human to achieve an NMSE score that was about 35% lower than the smallest score obtainable from the analog model. Nevertheless, we felt that the simplified representation of the controller was adequate for an investigation of switching effects.

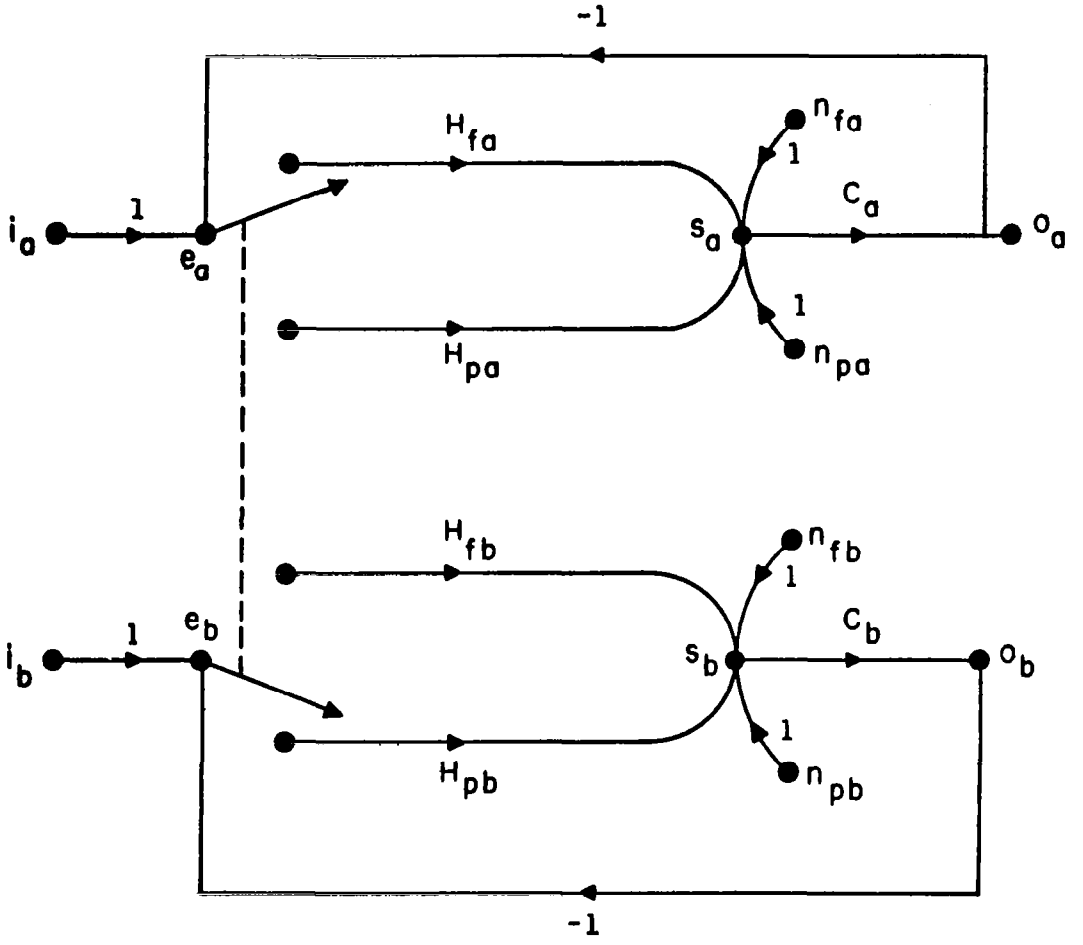

Fig. 20 Model of the 2-axis Manual Control Situation with Separated Displays

Input, system error, control stick motion, system output, and the human controller's remnant are indicated respectively by i, e, s, o, and n. H and C denote the human controller's describing function and the controlled-element dynamics. Foveal and peripheral strategies are denoted respectively by subscripts (f) and (p).

peripheral tracking performance with a display separation of 30^{o}. No remnant was simulated other than that due to switching effects.

The distribution of the total mean-squared error between the two axes was investigated as a function of the division of "foveal attention". The strategy-selector switch was driven by a periodic waveform unrelated to the forcing function, and the foveal dwell times on the two axes were varied in such a way that their sum was always 2.5 seconds. The forcing function was a 2 rad/sec waveform of the type used in the manual control experiments.

Figure 21 shows that the MSE obtained from the analog simulation is related to the allocation of foveal attention approximately as follows:

$$MSE_{2a} = A \cdot MSE_{fa} + (1-A)\ MSE_{pa} \qquad (9)$$

where A is the fraction of time that axis (a) is viewed foveally. This linear relationship implies that the total-task NMSE is independent of the division of attention and is equal to:

$$MSE_{1} = MSE_{2a} + MSE_{2b} = MSE_{f} + MSE_{p} \qquad (10)$$

when the control conditions are identical on both axes. When the conditions are different, the predicted total-task score is a linear function of the attentional division. In this situation, the lowest NMSE score will be obtained from the model when full foveal attention is devoted to the more difficult axis.

The applicability of these results to the manual control situation was determined by using the 1-axis foveal MSE scores, the 1-axis peripheral MSE scores, and the eye-movement data obtained in the manual control experiments to predict the 2-axis

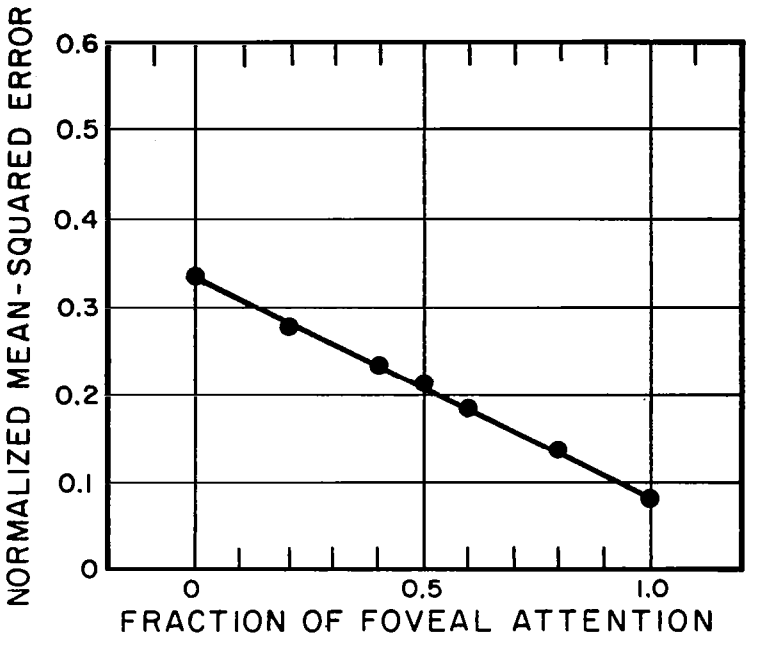

Fig. 21 Effect of Simulated Division of Attention on The Normalized Mean Squared Error Performance of One Axis of The Model

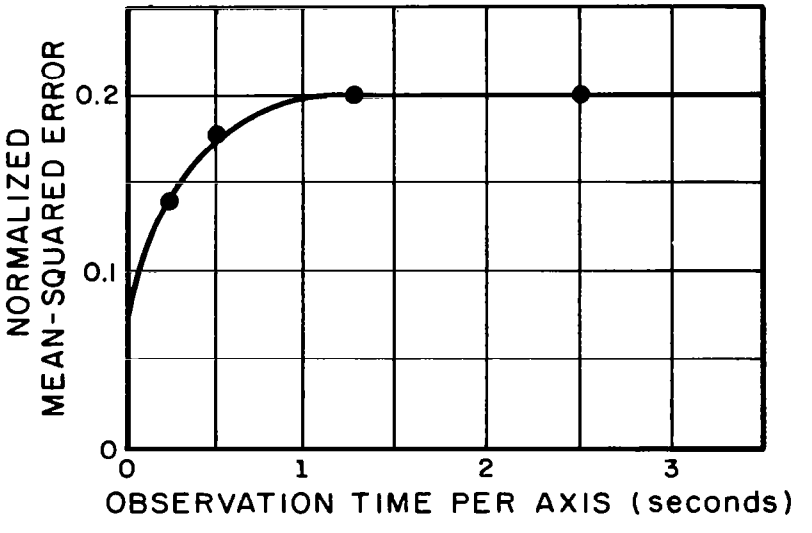

Fig. 22 Effect of Simulated Observation Time on The Normalized Mean Squared Error Performance of The Model

MSE scores according to equation (9). Table 14 shows that the predicted and measured average 2-axis scores generally differed by less than 10%. The greatest predictive errors occurred for the control situation in which the input bandwidths were different and the mean squared inputs were the same. The 2-axis MSE measured on the low-bandwidth axis was about three times that predicted by equation (2), whereas the MSE observed on the high-bandwidth axis was about 20% lower than the predicted score. The total-task MSE, however, was predicted with an error of less than 20%

An additional experiment was performed to show the effects of observation time on the NMSE performance of the model. The system was driven by the same 2 rad/sec signal used in the previous tests, and the foveal and peripheral "observation" times were identical in all runs. The NMSE remained at 0.2 as the observation time per axis was decreased from 2.5 to 1.25 sec and decreased as the observation time was further reduced (Figure 22). Extrapolation of the curve indicates that the NMSE score approaches the score obtained for full-time foveal tracking (0.08 for the model) as the observation time approaches zero.

Describing functions were obtained from the analog model for the following simulated tracking conditions: (1) 1-axis foveal, (2) 1-axis peripheral, and (3) 2-axis, with an even division of foveal attention between the two axes. A 2-rad/sec forcing function was used, and the dwell times were 1.25 sec for the 2-axis simulation.

The three describing functions had nearly identical shapes and differed only in gain (Figure 23). The peripheral gain was

TABLE 14

Predicted and Measured 2-Axis
Mean-Squared Errors Separated Displays

Experimental Variable	Predicted MSE (cm^2)	Measured MSE (cm^2)
a. Effects of Display Separation		
Separation = 30^o	.80	.76
Separation = 56^o	1.72	1.64
b. Effects of Input Bandwidth		
BW = 0.5 rad/sec	.77	.77
BW = 1.0 rad/sec	.77	.72
BW = 2.0 rad/sec	.84	.72
c. Different Bandwidths, Same MSI		
Low-bandwidth Axis	.11	.33
High-bandwidth Axis	.64	.52
Total Task	.75	.85
d. Different Bandwidths, Different MSI		
Low-bandwidth Axis	.43	.49
High-bandwidth Axis	.72	.61
Total Task	1.15	1.10
e. Effects of Controlled-Element Dynamics		
Dynamics = K	.52	.53
Dynamics = K/s	.77	.72
Dynamics = K/s^2	.80	1.00

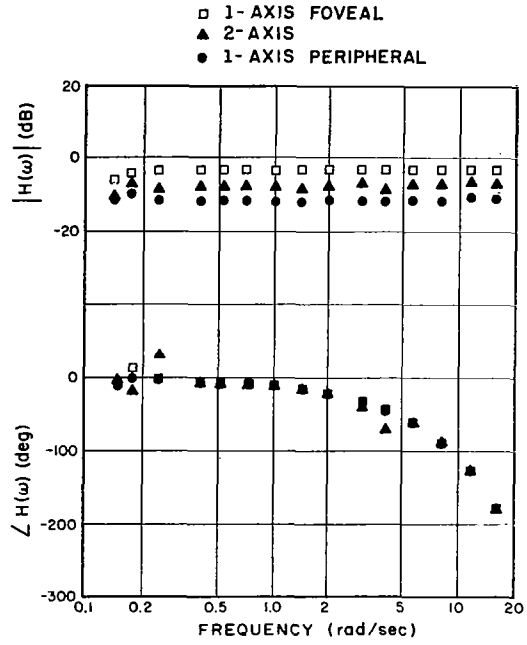

Fig. 23 Model Describing Functions for 1-axis Foveal, 1-axis Peripheral, and 2-axis Simulated Tracking Conditions

Controlled elements: K/s
Input bandwidths: 2 rad/sec
Simulated display separation: 30 degrees

8 dB less than the foveal gain, and the 2-axis gain was the average of the two 1-axis gains. The 2-axis model describing function, therefore, was related to the 1-axis describing functions in the same way as the human controller 2-axis describing functions were related to the corresponding 1-axis foveal and peripheral describing functions (Figure 12).

Although there was essentially no remnant associated with the 1-axis foveal or peripheral describing functions, the 2-axis simulation yielded a fractional "stick" remnant of 0.21. This remnant arose from the time-varying behavior of the model.

Because the NMSE and describing function measurements obtained from the analog system were similar in many respects to those obtained from the 2-axis manual control system, we conclude that the switched-strategy model of Figure 20 is a highly tenable one. It is intended only as a partial model of the control situation--one that provides reasonable predictions of the effects of instrument scanning on tracking performance.

2. Limitations of The Model

(a) An Inaccurate Prediction of The 2-Axis NMSE

When the tasks on the two axes were greatly different, the NMSE observed on the low-bandwidth axis was about three times as great as that predicted by the model. The following factors may have contributed to this discrepancy:

i. Peripheral non-linearities

The prediction of the low-bandwidth NMSE was based upon 1-axis scores obtained peripherally and foveally when the mean-squared input was 32 cm^2. The low-bandwidth MSI was only 4 cm^2, however, when the data under discussion were obtained. Because of the relatively large peripheral thresholds that we observed indirectly, we suspect that the effective peripheral gain decreased as the average amplitude of the displayed errors decreased. The controller's effective peripheral gain may, therefore, have been lower than that used in the analog simulation.*

ii. Non-stationarity of strategies

We have assumed that the peripheral and foveal strategies between which the controller switches in the 2-axis control situation are the same strategies employed when a single axis is tracked. (We do not yet have a method for measuring the individual strategies when two axes are tracked.) Since peripheral vision is affected by the entire visual scene, the subject's ability to track peripherally on Axis A may be degraded by activity on Axis B. This performance degradation would be more pronounced on the axis containing the least difficult task, since the ratio of foveal MSE to peripheral MSE is greater when the more difficult task is viewed foveally.

---

* We did not measure 1-axis peripheral tracking performance with an input signal having a cutoff of 0.5 rad/sec and an MSI of 4 cm^2.

(b) Inability to Predict Scanning Behavior

Modifications to the model of Figure 19 are necessary so that reasonable predictions of the controller's scanning behavior can be obtained. For example, the model predicts (1) that the NMSE will be progressively reduced as the scanning rate is increased without limit, (2) that the lowest NMSE score will be obtained if full foveal attention is paid to one axis when the conditions on the two axes are different, and (3) that the total-task NMSE will be independent of the scanning behavior when the control conditions are identical on the two axes. However, in our manual control experiments we found (1) that the mean observation time for a trial was rarely less than 1 sec., (2) that the subjects did not pay full attention to a single axis when the control conditions were different, and (3) that foveal attention was divided approximately evenly between the two axes when the control situation was homogeneous.

A cost associated with eye movements will lead to the prediction of a finite scanning rate. For example, let us assume that the rate of visual information obtained during eye movements is negligible compared to the information rates during foveal and peripheral viewing (Ref. 13). Thus, we assume that there is a fraction of the scanning period that is devoted neither to foveal or peripheral viewing--a period of visual dead time.

Let us assume that the tracking conditions are homogeneous and that the subject divides his useable attention equally between the two axes. Equation 9 may be modified to include the effects of dead time as follows:

$$NMSE_2 = \frac{(NMSE_f + NMSE_p)}{2}(1 - T_s/T_o) + \frac{T_s}{T_o}\frac{MSE_s}{MSI} \qquad (11)$$

where T_s is the time required for the eye to switch from one display to the other: T_o is the observation time for either foveal or peripheral viewing, and MSE_s is the mean-squared error associated with the visual dead time. T_o includes both the switching time T_s and the effective fixation time.

In order to place an upper bound on the effect of eye movements, we shall set $MSE_s = MSI$. That is, we shall assume that the input is effectively untracked during the visual dead time. The relation between the 2-axis NMSE score and observation time is given in Figure 24 for $NMSE_f = 0.05$, $NMSE_p = 0.35$ and $T_s = 0.1$ second--values that were typical of those observed during manual control. The NMSE decreases from 1.0 asymptotically to $(NMSE_f + NMSE_p)/2$ as T_o increases from T_s to an arbitrarily large value. An observation time of 1.25 sec results in an NMSE increase of 30% with respect to the minimum score of 0.2.

If we take account of the theoretical improvement obtainable with a relatively high scanning rate (Figure 22) the resulting NMSE scores will be lower than those shown in Figure 24 for $T_o > T_s$. The resulting NMSE-versus-T_o curve may show a minimum, depending on how the two effects combine. In any case, it is clear that the NMSE score must approach unity as the observation time approaches the visual dead time. The optimum scanning rate, therefore, must be finite.

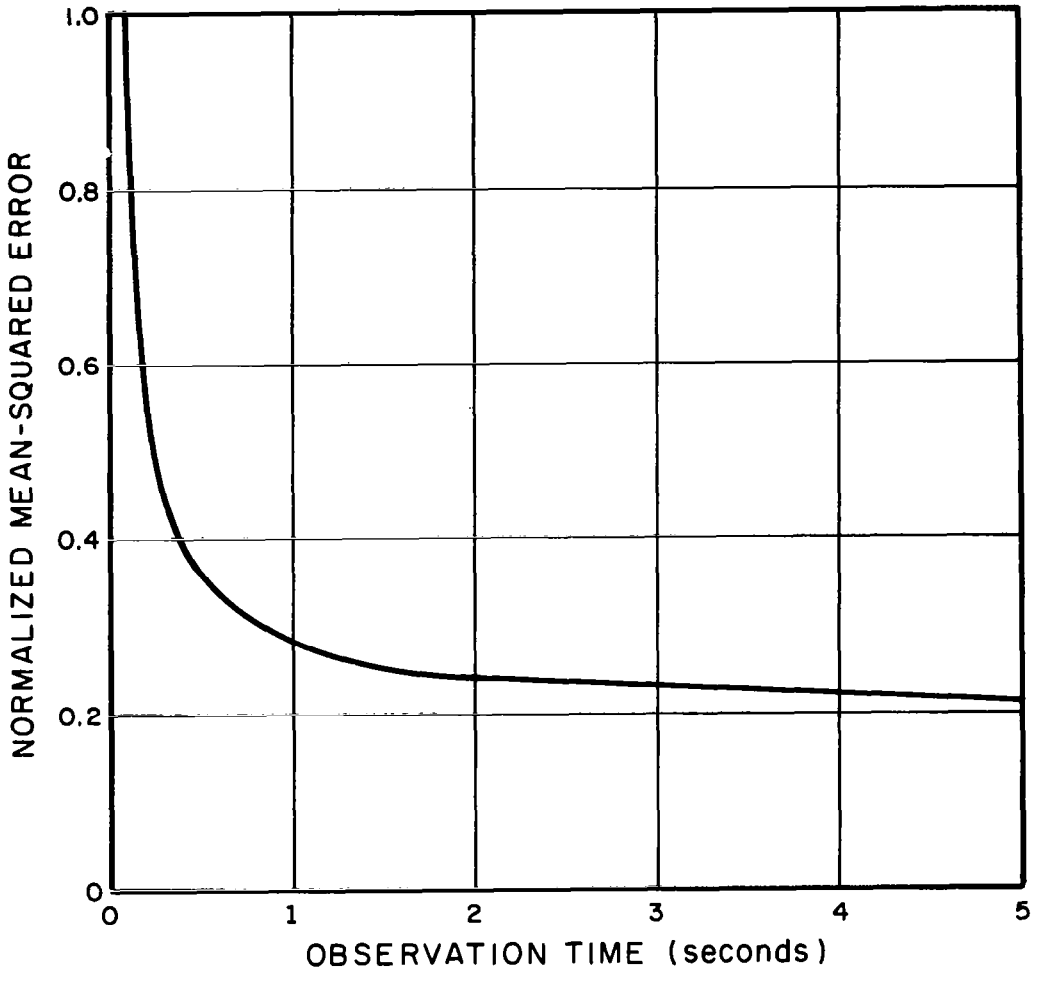

Fig. 24 Theoretical Effect of Observation Time on Normalized Mean Squared Error Performance When The Visual Dead Time Is 0.1 second.

The addition of a visual dead time to the model does not account for the subjects' tendency to allocate their attention equally between the two axes. Other mechanisms must be considered.

Because of their previous flight experience, the subjects may have adopted a secondary criterion of allocating their attention according to their estimate of the importance of the signals appearing on the two displays. Since we did not attempt to regulate the scanning behavior of the subjects, we do not know how the total-task NMSE score would have varied with changes in the allocation of attention.

C. Other Models

1. Pre-experiment Model

Prior to the experimental phase of this study, we postulated a model of the controller of a multi-axis system with separated displays and similar tasks on all axes. The model, discussed in detail in Reference 23, was based on the assumption that the controller would apply a zero-order hold to samples taken from the various displays and would apply a single continuous control strategy to each axis. Peripheral vision was not considered. The important predictions of the model were that the addition of a second axis of tracking would (a) quadruple the NMSE on each axis, (b) double the controller's effective time delay, and (c) decrease the controller's gain by 6 db.

The experimental results show that the basic premises of the original model are incorrect. The large increase in remnant in the 2-axis situation suggests an increase in the time-variability of the controller's describing function which is more consistent with a switched strategy than with a continuous strategy. The lack of a sizeable increase in time delay negates

the importance of zero-order holds. Furthermore, 2-axis performance appears to be intimately related to 1-axis peripheral performance. Because of the encouraging results obtained with the switched-strategy model of Figure 20, no further work has been done on the initial model.

2. Senders' Model of Monitoring Behavior

Equation 3 was used to predict the division of attention in the mixed-bandwidth, identical-MSI condition of Experiment 3 from the error scores that were obtained experimentally (Table A12). The error bandwidths were assumed equal to the input bandwidths, K was assumed equal to 0.5 seconds/bit (based on typical 1-axis information processing rates reported in Reference 10), and C was set equal to 0.1 sec (approximate switching time between displays separated by 30 degrees). The predictions were inconsistent with the measured attentional division. The predicted fractional allocation of foveal attention was 0.53 on the high-bandwidth axis and 0.16 on the low-bandwidth axis, whereas the measured division of attention was 0.63, 0.37. Not only do the fractional allocations not sum to unity, but the predicted ratio of high-bandwidth attention to low-bandwidth attention is about twice that observed experimentally.

Obviously, this model needs further development before it can be used to predict monitoring behavior in a multi-axis control situation. The model does not assure that the sum of the fractional allocations of attention will sum to unity.*

---

* This is an essential feature of the model as originally intended. A sum greater than unity is to be interpreted as an intolerably high workload on the observer. A sum less than unity implies that the observer can perform satisfactorily.

In addition, reliable estimates are needed for constants K and C and for the error bandwidth, which need not be identical to the input bandwidth in a closed-loop system.

D. Further Model Development

A suitable model of the controller's scanning behavior must be developed before a unified model of the multi-axis control situation can be constructed. Such a model might consist of an optimization procedure that interacts with a model of the type discussed in Section B to determine the scanning pattern that will minimize a specified cost function. Physiological and psychological factors that limit the scanning rate will have to be considered. Experiments that are designed to test such models should employ performance criteria such that the performance score will be a sensitive indicator of deviations from optimum scanning behavior.

We have shown in our studies of two-axis systems that peripheral vision plays an important role. However, as we go to higher-dimensional tasks, the complexity of the visual field may be so great that the relative contribution of peripheral tracking in any one control loop will be small. If this turns out to be the case, we may be able to simplify the structure of the multi-axis model by considering only foveal monitoring and control behavior.

REFERENCES

1. Elkind, J. I., Characteristics of Simple Manual Control Systems, MIT, Lincoln Laboratory, TR-111, 6 April 1956.

2. McRuer, D. T. and E. S. Krendel, Dynamic Response of Human Operators, WADC-TR-56-524, October 1957.

3. McRuer, D. T., Graham, D., Krendel, E. S. and Reisener, W., Jr., Human Pilot Dynamics in Compensatory Systems, Theory, Models, and Experiments with Controlled Element and Forcing Function Variations, AFFDL-TR-65-15, July 1965.

4. Fitts, P. M. and Simon, C. W. (1949): Effect of Horizontal vs Vertical Stimulus Separation on Performance in a Dual Pursuit Task. Amer. Psychologist 4; 304-305.

5. Chernikoff, R., et al, Two-Dimensional Tracking with Identical and Different Control Dynamics in Each Coordinate, NRL Rpt. 5424, 27 November 1959.

6. Duey, J. W. and Chernikoff, R., The Use of Quickening in One Coordinate of a Two-Dimensional Tracking System, IEEE Trans., HFE-1, 21-24, March 1960.

7. Chernikoff, R. and LeMay, M., Effect of Various Display-Control Configurations on Tracking with Identical and Different Coordinate Dynamics, J. Exper. Psych., Vol. 66, No. 1, 95-99, 1963.

8. Verdi, A. P., et al, Effects of Display Quickening on Human Transfer Functions During a Dual-Axis Compensatory Tracking Task, ASD-TDR-65, BSL, WPAFB, March 1965.

9. Todosiev, E. P., Rose, R. E., Bekey, G. A. and Williams, H. L., Human Tracking Performance in Uncoupled and Coupled Two-Axis Systems, TRW Systems, 4380-6003-R0000, 8 December 1965.

10. Levison, W. H, and Elkind, J. I., Studies of Multi-Variable Manual Control Systems: Two-Axis Compensatory Systems With Compatible Integrated Display and Control, BBN Report No. 1339, January 1966.

11. Wierwille, W. W. and G. A. Gagne, Nonlinear and Time-Varying Dynamical Models of Human Operators in Manual Control Systems, Human Factors, 8:97-120, April 1966.

12. Senders, J. W., Elkind, J. I., Grignetti, M. C. and Smallwood, R. D., An Investigation of the Visual Sampling Behavior of Human Observers, NASA Report No. CR-434, pp. 27-33, April 1966.

13. Sanders, A. F., The Selective Process in the Functional Visual Field, Van Gorcum & Comp. N.V., Amsterdam, the Netherlands, 1963.

14. Senders, J. W., Webb, E. B., and Baker, C. A., The Peripheral Viewing of Dials, The Journal of Applied Psychology, Vol. 39, No. 6, 1955.

15. McColgin, F. H., Movement Thresholds In Peripheral Vision. Journal of the Optical Society of America, Vol. 50, 774-779, August 1960.

16. Graham, C. H. (ed.), Vision and Visual Perception, Wiley and Sons, N. Y., 1965.

17. Kris, E. C., A Technique for Electrically Recording Eye Position, WADC Tech. Rpt. 58-660, Wright-Patterson Air Force Base, December 1958.

18. Winer, B. J., Statistical Principles in Experimental Design. McGraw-Hill, 1962.

19. Tustin, A., "The Nature of the Operator's Response in Manual Control and Its Implications for Controller Design," J. of the IEEE Vol. 94 Part IIA, No. 2, 1947.

20. Taylor, Lawrence W., Jr., "Discussion of Spectral Human-Response Analysis," NASA Flight Research Center.

21. Cooley, J. W. and J. W. Tukey, "An Algorithm for the Machine Calculation of Complex Fourier Series," Mathematics of Computation 10, No. 90, pp 297-301, April 1965.

22. Fitts, P. M., et al, "Eye fixations of aircraft pilots: Frequency, duration, and sequence of fixations when flying Air Force ground controlled approach system (GCA)," AF Tech. Rept. 5967 (ATI 69038), February 1950.

23. Bolt Beranek and Newman Inc., "Studies of Manual Control Systems", Progress Report No. 2, March 1966, Job No. 11215.

24. Senders, J. W., Personal Communication.

25. Grignetti, M.C., with Payne, R.V. and Elkind, J.I., "Signal Analyzer I. A Signal Analysis System for Manual Control Studies" IEEE Int. Convention Record 13: 143-151, Part 6, 1965.

APPENDIX A:

TABLE A1

NMSE Scores for Preliminary Experiments
(average of 2 trials)

	V-Axis		H-Axis		Total Task	
Subject	1-Axis	2-Axis	1-Axis	2-Axis	1-Axis	2-Axis
JF	.0577	.183	.0687	.262	.0636	.222
DM	.0547	.187	.0547	.205	.0550	.196
PM	.0670	.193	.0707	.289	.0687	.241
CR	.0713	.256	.0790	.316	.0753	.280
4 Subjects	.0627	.205	.0682	.268	.0657	.236

TABLE A2

Summary of Analysis of Variance of
NMSE Scores For Preliminary Experiment

a. Number X Subject

	Significance Level		
Source	L Axis (vert)	R Axis (horiz)	Total Task
Number of Axes	.01	.01	.01
Subject	--	--	--
Subject X Number	.05	.05	.01

b. Axis X Subject

	Significance Level	
Source	1-Axis	2-Axis
Axis	.01	.01
Subject	.001	.001
Subject X Axis	---	---

TABLE A3

Mean Observation Time, Allocation of Foveal Attention, and Division of 2-Axis NMSE for Preliminary Experiment (average of two trials)

	Mean Observation Time (sec)			Fractional Allocations			
				Foveal Attn.		2-Axis NMSE	
Subject	L Axis	R Axis	Avg	L Axis	R Axis	L Axis	R Axis
JF	1.1	1.5	1.3	0.42	0.58	0.41	0.59
DM	1.3	1.3	1.3	0.49	0.51	0.48	0.52
PM	0.9	1.5	1.2	0.39	0.62	0.40	0.60
CR	0.8	1.2	1.0	0.40	0.60	0.45	0.55
4 Subjects	1.0	1.4	1.2	0.42	0.58	0.44	0.56

TABLE A4

Effect of Display Separation on The NMSE Scores

	Display Separation					
	1-axis foveal	1-axis peripheral		2-axis		
Subject	0°	30°	56°	0.8°	30°	56°
			a. Left Axis			
JF	.0335	.325	.708	.0455	.205	.542
DM	.0440	--	--	.0735	.181	.388
PM	.0530	.310	.732	.0855	.189	.350
CR	.0495	.306	.956	.0567	.166	.408
Average	.0450	.314	.799	.0653	.185	.422
			b. Right Axis			
JF	.0375	.416	1.09	.0580	.166	.417
DM	.0540	--	--	.0695	.174	.513
PM	.0625	.390	.722	.0995	.179	.329
CR	.0695	.385	.666	.0960	.225	.449
Average	.0559	.397	.799	.0808	.186	.427
			c. Total Task			
JF	.0350	.371	.858	.0515	.186	.466
DM	.0485	--	--	.0710	.178	.451
PM	.0575	.350	.727	.0930	.183	.339
CR	.0600	.346	.811	.0770	.196	.429
Average	.0503	.356	.799	.0731	.186	.421

Controlled-element Dynamics = K/s

Input Bandwidth = 2 rad/sec

Average of 2 trials for 1-axis foveal and 2-axis entries

Average of 3 trials for 1-axis peripheral entries

TABLE A5

Summary of Analysis of Variance of
NMSE Scores For Experiment 1

Source	Significance Levels L Axis	R Axis	Total Task
a. Display Separation = 0.8°			
Number of Axes	.001	.001	.001
Subject	.01	.01	.001
Number X Subject	--	--	--
b. Display Separation = 30°			
Number of Axes	.001	.001	.001
Subject	--	.01	--
Number X Subject	--	--	--
c. Display Separation = 56°			
Number of Axes	.01	.001	.001
Subject	--	--	--
Number X Subject	.05	--	--

TABLE A6

Effect of Display Separation On
Fractional Remnant Power
Right Axis

	Display Separation					
	1-axis foveal	1-axis peripheral		2-axis		
Subject	0^{o}	30^{o}	56^{o}	0.8^{o}	30^{o}	56^{o}
			a. Stick			
JF	.18	.57	.70	.21	.50	.72
DM	.20	--	--	.19	.33	.49
PM	.15	.50	.68	.20	.36	.47
CR	.14	.36	.57	.16	.40	.46
Average	.17	.48	.65	.19	.40	.54
			b. Error			
JF	.30	.74	.79	.36	.62	.67
DM	.38	--	--	.33	.52	.62
PM	.29	.78	.57	.34	.48	.50
CR	.35	.58	.64	.33	.48	.52
Average	.33	.70	.67	.34	.53	.58

Average of 2 trials for 1-axis foveal and 2-axis entries
Average of 3 trials for 1-axis peripheral entries

TABLE A7

Effect of Display Separation on Mean Observation Time, Allocation of Foveal Attention, and Division of 2-axis MSE

Subject	Mean Observation Time (sec)			Fractional Allocations Foveal Attn.		2-axis NMSE	
	L Axis	R Axis	Avg.	L Axis	R Axis	L Axis	R Axis
			a. Display Separation = 30°				
JF	0.8	1.2	1.0	.42	.58	.55	.45
DM	1.1	1.4	1.3	.44	.56	.51	.49
PM	1.1	2.0	1.6	.35	.65	.50	.50
CR	0.8	1.2	1.0	.39	.61	.41	.59
Average	1.0	1.4	1.2	.40	.60	.49	.51
			b. Display Separation = 56°				
JF	0.9	1.3	1.1	.41	.59	.57	.43
DM	1.4	1.8	1.6	.43	.57	.43	.54
PM	1.0	1.6	1.3	.39	.61	.50	.50
CR	1.0	1.5	1.3	.40	.60	.46	.54
Average	1.1	1.6	1.3	.41	.59	.49	.51

Average of 2 trials

TABLE A8

Effect of Input Bandwidth on The NMSE Scores

	Input Bandwidth (rad/sec)								
	1-axis foveal			1-axis periph.			2-axis		
Subject	0.5	1.0	2.0	0.5	1.0	2.0	0.5	1.0	2.0
	a. Left Axis								
JF	.0082	.0148	.0407	.0296	.0784	.325	.0240	.0519	.201
DM	.0123	.0228	.0493	.0345	.0694	--	.0245	.0464	.166
PM	.0109	.0193	.0580	.0318	.0536	.310	.0242	.0453	.210
Average	.0104	.0189	.0493	.0320	.0671	--	.0242	.0478	.192
	b. Right Axis								
JF	.0106	.0181	.0410	.0392	.102	.416	.0219	.0416	.141
DM	.0111	.0195	.0484	.0435	.0780	--	.0249	.0422	.178
PM	.0125	.0230	.0658	.0409	.0705	.390	.0251	.0455	.182
Average	.0114	.0202	.0517	.0411	.0836	--	.0239	.0431	.169
	c. Total Task								
JF	.0094	.0165	.0408	.0344	.0902	.371	.0229	.0466	.168
DM	.0117	.0211	.0488	.0390	.0737	--	.0247	.0443	.172
PM	.0116	.0212	.0622	.0363	.0621	.350	.0246	.0452	.194
Average	.0109	.0196	.0506	.0366	.0753	--	.0241	.0454	.178

Controlled-element Dynamics = K/s

Display Separation = 30°

Average of 2 trials for 1-axis foveal and 2-axis entries

Average of 3 trials for 1-axis peripheral entries

TABLE A9

Summary of Analysis of Variance of
NMSE Scores For Experiment 2

Source	Significance Level L Axis	R Axis	Total Task
a. Input Bandwidth = 0.5 rad/sec			
Number of Axes	.001	.001	.001
Subject	---	---	---
Number X Subject	---	---	---
b. Input Bandwidth = 1.0 rad/sec			
Number	.001	.001	.001
Subject	---	---	---
Number X Subject	---	---	---
c. Input Bandwidth = 2.0 rad/sec			
Number	.001	.001	.001
Subject	---	.01	.001
Number X Subject	---	---	---

TABLE A-10

Effect of Input Bandwidth on Fractional Remnant Power
Right Axis

	Input Bandwidth (rad/sec)								
	1-axis foveal			1-axis periph.			2-axis		
Subject	0.5	1.0	2.0	0.5	1.0	2.0	0.5	1.0	2.0
a. Stick									
JF	.22	.22	.21	.59	.56	.57	.41	.42	.40
DM	.13	.13	.13	.49	.32	--	.27	.28	.30
PM	.12	.13	.17	.53	.44	.50	.34	.28	.32
Average	.16	.16	.17	.54	.44	--	.34	.33	.34
b. Error									
JF	.24	.27	.28	.66	.62	.74	.47	.56	.55
DM	.16	.20	.24	.67	.70	--	.47	.53	.48
PM	.20	.21	.28	.73	.70	.78	.44	.43	.42
Average	.20	.23	.27	.69	.67	--	.46	.51	.48

Average of 2 trials for 1-axis foveal and 2-axis entries
Average of 3 trials for 1-axis peripheral entries

TABLE A-11

Effect of Input Bandwidth on Mean Observation Time, Allocation of Foveal Attention, and Division of 2-axis MSE

Subject	Mean Observation Time (sec)			Fractional Allocations			
				Foveal Attn.		2-axis NMSE	
	L Axis	R Axis	Avg	L Axis	R Axis	L Axis	R Axis
a. Input Bandwidth = 0.5 rad/sec							
JF	1.18	1.48	1.33	.44	.56	.52	.48
DM	1.25	1.57	1.41	.44	.56	.50	.50
PM	1.16	1.85	1.50	.38	.62	.49	.51
Average	1.20	1.63	1.41	.42	.58	.50	.50
b. Input Bandwidth = 1.0 rad/sec							
JF	1.17	1.47	1.32	.44	.56	.56	.44
DM	1.11	1.44	1.28	.44	.56	.52	.48
PM	1.06	1.63	1.34	.39	.61	.50	.50
Average	1.11	1.51	1.31	.42	.58	.53	.47
c. Input Bandwidth = 2.0 rad/sec							
JF	1.05	1.61	1.33	.40	.60	.59	.41
DM	1.19	1.44	1.31	.45	.55	.48	.52
PM	1.36	1.67	1.52	.39	.61	.54	.46
Average	1.20	1.57	1.39	.41	.59	.53	.47

Average of 2 trials

TABLE A-12

Effect of Axis Differences on the MSE and NMSE Scores

Subject	ω_i=0.5 rad/sec 1-axis	ω_i=0.5 rad/sec 2-axis	ω_i=2 rad/sec 1-axis	ω_i=2 rad/sec 2-axis	Total Task 1-axis	Total Task 2-axis
a. Same Mean-squared Inputs to Both Axes						
	Normalized Mean-squared Error					
JF	.00796	.0676	.0360	.121	.0220	.0943
DM	.0104	.0796	.0508	.134	.0306	.107
PM	.0119	.101	.0554	.127	.0332	.114
Average	.0101	.0828	.0474	.127	.0286	.105
b. Different Mean-squared Inputs to the Two Axes						
	Mean-squared Error (cm^2)					
JF	.163	.468	.170	.522	.166	.494
DM	.201	.516	.225	.651	.218	.583
PM	.208	.499	.228	.658	.218	.578
Average	.190	.494	.207	.609	.199	.552

Controlled-element Dynamics = K/s
Display Separation = 30^o
Average of 4 trials

TABLE A-13

Summary of Analysis of Variance of
NMSE Scores For Experiment 3

Source	Significance Level ω_i=0.5 rad/sec	ω_i=2 rad/sec	Total Task
a. Same Mean-squared Inputs to Both Axes			
Number of Axes	.001	.001	.001
Subject	.05	.01	.01
Number X Subject	--	--	--
b. Different Mean-squared Inputs to Each Axis			
Number of Axes	.001	.001	.001
Subject	--	.01	.05
Number X Subject	--	--	--

TABLE A-14

Effect of Axis Differences on Fractional Remnant Power

Right Axis

Subject	Same MSI on Both Axes				Different MSI*	
	1-axis		2-axis		2-axis	
	ω_i=0.5	ω_i=2	ω_i=0.5	ω_i=2	ω_i=0.5	ω_i=2
a. Stick						
JF	.27	.16	.65	.36	.50	.40
DM	.19	.15	.54	.27	.34	.25
PM	.18	.14	.57	.28	.39	.41
Average	.21	.15	.59	.30	.41	.35
b. Error						
JF	.31	.23	.68	.49	.58	.54
DM	.28	.29	.55	.43	.47	.39
PM	.27	.27	.65	.39	.52	.50
Average	.29	.26	.63	.44	.52	.46

* 1-axis remnant not computed for this experiment
Average of 2 trials.

TABLE A-15

Effect of Axis Differences on Mean Observation Time, Allocation of Foveal Attention, and Division of 2-axis MSE

	Mean Observation Time (sec)		Fractional Allocations Foveal Attn.		2-axis NMSE	
Subject	ω_i=0.5	ω_i=2	ω_i=0.5	ω_i=2	ω_i=0.5	ω_i=2
a. Same Mean-squared Inputs to Both Axes						
JF	1.24	1.64	.43	.57	.36	.64
DM	0.96	1.78	.35	.65	.37	.63
PM	1.25	2.70	.32	.68	.44	.56
Average	1.15	2.04	.37	.63	.39	.61
b. Different Mean-squared Inputs to Each Axis						
JF	1.32	1.56	.46	.54	.47	.53
DM	1.20	1.34	.47	.53	.44	.56
PM	1.32	2.33	.36	.64	.43	.57
Average	1.28	1.74	.43	.57	.45	.55

Average of 4 trials

TABLE A-16

Effect of Controlled element Dynamics on the NMSE Scores

Subject	Controlled-element Dynamics: 1-axis foveal K	1-axis foveal K/s	1-axis foveal K/s^2	1-axis periph. K	1-axis periph. K/s	1-axis periph. K/s^2	2-axis K	2-axis K/s	2-axis K/s^2
a. Left Axis									
JF	.0143	.0148	.0409	.0732	.0784	.378	.0488	.0519	.308
DM	.0213	.0228	.0573	.0942	.0694	.221	.0511	.0464	.187
PM	.0209	.0193	.0613	.0671	.0536	.374	.0585	.0453	.291
Avg.	.0188	.0189	.0532	.0778	.0671	.324	.0528	.0478	.262
b. Right Axis									
JF	.0161	.0181	.0513	.0101	.0102	.418	.0448	.0416	.362
DM	.0181	.0195	.0467	.0733	.0780	.267	.0589	.0422	.181
PM	.0197	.0230	.0536	.0995	.0705	.379	.0572	.0455	.240
Avg.	.0180	.0202	.0505	.0914	.0836	.355	.0536	.0431	.294
c. Total Task									
JF	.0152	.0165	.0460	.0869	.0902	.398	.0468	.0466	.335
DM	.0198	.0211	.0521	.0838	.0737	.244	.0550	.0443	.184
PM	.0203	.0212	.0575	.0833	.0621	.377	.0579	.0452	.266
Avg.	.0184	.0196	.0519	.0846	.0753	.340	.0532	.0454	.261

Input Bandwidth = 1 rad/sec
Display Separation = 30^{o}
Average of 2 trials for 1-axis foveal and 2-axis entries
Average of 3 trials for 1-axis peripheral entries

TABLE A-17

Summary of Analysis of Variance of NMSE Scores
For Experiment 4

Source	Significance Level L Axis	R Axis	Total Task
a. Controlled-Element Dynamics = K			
Number of Axes	.001	.001	.001
Subject	---	.05	.05
Number X Subject	---	---	---
Average	---	---	---
b. Controlled-Element Dynamics = K/s			
Number of Axes	.001	.001	.001
Subject	---	---	---
Number X Subject	---	---	---
Average	---	---	---
c. Controlled-Element Dynamics = K/s^2			
Number of Axes	.001	---	.05
Subject	---	---	---
Number X Subject	---	.01	.05
Average	---	---	---

TABLE A-18

Effect Of Controlled-Element Dynamics On
Fractional Remnant Power

Right Axis

	Controlled-element Dynamics								
		1-axis foveal			1-axis peripheral			2-axis	
Subject	K	K/s	K/s^2	K	K/s	K/s^2	K	K/s	K/s^2
a. Stick									
JF	.035	.22	.45	.15	.56	.86	.076	.42	.85
DM	.031	.13	.39	.053	.32	.79	.079	.28	.77
PM	.029	.13	.52	.048	.44	.88	.039	.28	.78
Avg.	.032	.16	.45	.084	.44	.84	.055	.33	.80
b. Error									
JF	.36	.27	.53	.60	.62	.74	.50	.56	.81
DM	.25	.20	.34	.43	.70	.67	.48	.53	.54
PM	.23	.21	.50	.62	.70	.77	.33	.43	.73
Avg.	.28	.23	.46	.55	.67	.73	.44	.51	.69

Average of 2 trials for 1-axis foveal and 2-axis entries
Average of 3 trials for 1-axis peripheral entries

"The aeronautical and space activities of the United States shall be conducted so as to contribute . . . to the expansion of human knowledge of phenomena in the atmosphere and space. The Administration shall provide for the widest practicable and appropriate dissemination of information concerning its activities and the results thereof."

—NATIONAL AERONAUTICS AND SPACE ACT OF 1958

NASA SCIENTIFIC AND TECHNICAL PUBLICATIONS

TECHNICAL REPORTS: Scientific and technical information considered important, complete, and a lasting contribution to existing knowledge.

TECHNICAL NOTES: Information less broad in scope but nevertheless of importance as a contribution to existing knowledge.

TECHNICAL MEMORANDUMS: Information receiving limited distribution because of preliminary data, security classification, or other reasons.

CONTRACTOR REPORTS: Scientific and technical information generated under a NASA contract or grant and considered an important contribution to existing knowledge.

TECHNICAL TRANSLATIONS: Information published in a foreign language considered to merit NASA distribution in English.

SPECIAL PUBLICATIONS: Information derived from or of value to NASA activities. Publications include conference proceedings, monographs, data compilations, handbooks, sourcebooks, and special bibliographies.

TECHNOLOGY UTILIZATION PUBLICATIONS: Information on technology used by NASA that may be of particular interest in commercial and other non-aerospace applications. Publications include Tech Briefs, Technology Utilization Reports and Notes, and Technology Surveys.

Details on the availability of these publications may be obtained from:

SCIENTIFIC AND TECHNICAL INFORMATION DIVISION

NATIONAL AERONAUTICS AND SPACE ADMINISTRATION

Washington, D.C. 20546